Journal of Human Evolution 157 (2021) 103028

Contents lists available at ScienceDirect

Journal of Human Evolution

journal homepage: www.elsevier.com/locate/jhevol

Eastern African environmental variation and its role in the evolution and cultural change of *Homo* over the last 1 million years

Rachel L. Lupien [a, b, *], James M. Russell [a], Avinash Subramanian [a], Rahab Kinyanjui [c], Emily J. Beverly [d], Kevin T. Uno [b], Peter de Menocal [e, b], René Dommain [f, g], Richard Potts [g, c]

[a] Department of Earth, Environmental, and Planetary Sciences, Brown University, Providence, RI 02906, USA
[b] Division of Biology and Paleo Environment, Lamont-Doherty Earth Observatory, Palisades, NY 10964, USA
[c] Department of Earth Sciences, National Museums of Kenya, Nairobi 00100, Kenya
[d] Department of Earth and Atmospheric Sciences, University of Houston, Houston, TX 77204, USA
[e] Woods Hole Oceanographic Institution, Woods Hole, MA 02543, USA
[f] Institute of Geosciences, University of Potsdam, 14476 Potsdam, Germany
[g] Human Origins Program, National Museum of Natural History, Smithsonian Institution, Washington, DC 20560, USA

ARTICLE INFO

Article history:
Received 17 November 2020
Accepted 20 May 2021
Available online xxx

Keywords:
Human evolution
Paleoclimate
East Africa
Organic geochemistry
Biomarkers
Carbon isotopes

ABSTRACT

Characterizing eastern African environmental variability on orbital timescales is crucial to evaluating the hominin evolutionary response to past climate changes. However, there is a dearth of high-resolution, well-dated records of ecosystem dynamics from eastern Africa that cover long time intervals. In the last 1 Myr, there were significant anatomical and cultural developments in *Homo*, including the origin of *Homo sapiens*. There were also major changes in global climatic boundary conditions that may have affected eastern African environments, yet potential linkages remain poorly understood. We developed carbon isotopic records from plant waxes ($\delta^{13}C_{wax}$) and bulk organic matter ($\delta^{13}C_{OM}$) from a well-dated sediment core spanning the last ~1 Myr extracted from the Koora Basin, located south of the Olorgesailie Basin, in the southern Kenya rift. Our record characterizes the climatic and environmental context for evolutionary events and technological advances recorded in the adjacent Olorgesailie Basin, such as the transition from Acheulean to Middle Stone Age tools by 320 ka. A significant shift toward more C_4-dominated ecosystems and arid conditions occurred near the end of the mid-Pleistocene Transition, which indicates a link between equatorial eastern African and high-latitude northern hemisphere climate. Environmental variability increases throughout the mid- to late-Pleistocene, superimposed by precession-paced packets of variability modulated by eccentricity. An interval of particularly high-amplitude climate and environmental variability occurred from ~275 ka to ~180 ka, synchronous with evidence for the first *H. sapiens* fossils in eastern Africa. These results support the 'variability selection hypothesis' that increased environmental variability selected for adaptable traits, behaviors, and technology in our hominin ancestors.

1. Introduction

Eastern Africa experienced dramatic environmental changes during the Quaternary, and these high-amplitude climatic and environmental fluctuations may have played a key role in favoring evolutionary changes in our hominin ancestors (deMenocal, 1995; Tierney et al., 2017). These include increased hominin mobility and cognitive capacity that allowed some hominins to survive and reproduce in a wider range of ecosystems (Roberts and Stewart, 2018). Understanding past variability in hominin habitats is crucial for testing evolutionary hypotheses but is hampered by the lack of long, continuous, well-dated environmental records that can resolve the full range of environmental fluctuations potentially related to multigenerational periods over which evolutionary changes occur.

* Corresponding author.
E-mail address: rlupien@ldeo.columbia.edu (R.L. Lupien).

https://doi.org/10.1016/j.jhevol.2021.103028
0047-2484/

Previous work quantifying multimillion-year changes in eastern African vegetation suggests that C_4 grasslands gradually expanded in the region since the Miocene (Feakins et al., 2013; Uno et al., 2016a; Polissar et al., 2019). Soil carbonate carbon isotope data ($\delta^{13}C_{SC}$) from the Tugen Hills (Cerling, 1992; Kingston, 1992), Afar (Levin et al., 2004; Quade et al., 2004; Yellen et al., 2005; WoldeGabriel et al., 2009; Cerling et al., 2011), Omo-Turkana (Levin et al., 2011), Olorgesailie (Sikes et al., 1999), and Oldupai (formerly Olduvai; Cerling and Hay, 1986) Basins document this regional expansion (Levin, 2013, 2015), including during the last 1 Myr. However, it is difficult to extract orbital-scale variability from these records, and there are significant differences in the rates, amplitudes, and timing of ecological change between these basins, potentially because of local climate differences and/or the local geomorphological evolution of each basin (Olaka et al., 2010). These differences highlight the need for higher resolution records to understand large-scale climate changes in eastern Africa during the Quaternary and to examine the basin-scale environmental changes experienced by early hominins.

Monsoon-driven hydroclimate variability is a key control on ecosystem variability in eastern Africa (Kutzbach et al., 2020) and has been shown to fluctuate primarily in response to variations in low-latitude summer insolation (e.g., Kutzbach, 1981; Kutzbach and Otto-Bliesner, 1982; Joordens et al., 2011; Colcord et al., 2018; Lupien et al., 2018; Nutz and Schuster, 2018). Incoming solar radiation (insolation) directly controls the monsoons at low latitudes and also controls many components of the climate system (Milankovitch, 1941) that may directly or indirectly influence the monsoons (deMenocal, 1995), including high-latitude insolation-driven ice volume (Hays et al., 1976), ocean circulation (Ruddiman et al., 1989), greenhouse gas concentration (Petit et al., 1999), sea surface temperature (SST; Herbert et al., 2010), and SST gradients (Broccoli et al., 2006; Brierley and Fedorov, 2010). Many of these climate system components have changed substantially over the last 1 Myr, for instance, during the mid-Pleistocene transition (MPT) ~1250–700 ka, when glacial–interglacial variability transitioned from obliquity-paced (~41 kyr; axial tilt) to lower frequency (80–120 kyr) cycles while also increasing in amplitude (Clark et al., 2006). Ice volume cycles and atmospheric greenhouse gas variations subsequently intensified again at the mid-Brunhes Event (MBE) at ~430 ka (Jansen et al., 1986; EPICA Team Members, 2004). There is evidence of changes in North African land surface processes associated with high-latitude climate transitions (deMenocal, 1995), yet we continue to lack adequate records from tropical eastern Africa to examine low-latitude environmental responses in the locations where early hominins lived and evolved.

If African environments responded to both low-latitude insolation forcing and high-latitude climate transitions, we would expect hominin lineages to have experienced changes in regional climate variability across seasonal to orbital time scales associated with the East African Monsoon, as well as long-term or step changes in mean climate and climate variability driven by high-latitude teleconnections. Understanding these climatic and environmental responses would make important predictions for environmental factors that influenced human evolutionary history. To quantify environmental variation in eastern Africa and to help determine the controls on regional ecosystem change and hominin evolution, we present records of carbon isotopes from both plant waxes and bulk organic matter (OM) from a long, well-dated sediment core from southern Kenya that spans the last 1 Myr.

1.1. Study site

The sediment core record presented here is from the Koora Basin, an adjacent sedimentary basin to the famous fossil and archeological site of Olorgesailie. The Olorgesailie Basin (Fig. 1) has a long history of paleontological and paleoanthropological research that has recorded numerous archeological sites and tens of thousands of stone artifacts and fossil animal remains (e.g., Isaac and Isaac, 1977; Potts et al., 1999; Potts et al., 2018). Outcrops in the basin have provided unparalleled stratigraphic context for hominin morphological and behavioral transitions, particularly over the past 1 Myr (Deino and Potts, 1990; Potts, 1994; Behrensmeyer et al., 2002, 2018; Potts et al., 2018). Olorgesailie documents the earliest evidence of the transition from Acheulean stone tools (e.g., large, bifacial handaxes) to the smaller, more complex tools of the middle stone age (MSA) in eastern Africa by ~320 ka (Deino et al., 2018). Furthermore, evidence of long-distance obsidian transfer and pigment use from this region mark advances in social and cultural behavior (Brooks et al., 2018). The changes toward these behaviors linked to early *Homo sapiens* occurred between 500 ka and 320 ka, an interval of time not captured by the outcrop record because of an erosional hiatus (Behrensmeyer et al., 2018). Other issues associated with outcrop archives, such as oxidation of organic compounds, have further limited characterization of Olorgesailie paleoenvironments.

Drilling sites in the Koora Basin were located 24 km south and downstream of Olorgesailie Basin outcrops in the southern Kenya rift, and the two basins shared episodic depositional connectivity (Fig. 1). Sediment cores were recovered in 2012 in the Koora Basin as part of the Olorgesailie Drilling Project (ODP). The cores provide a continuously deposited archive (ODP-OLO12-1A; 1.79 °S, 36.40 °E; Potts et al., 2020), including sediment spanning the 500–320 ka outcrop hiatus. The 139-m drill core, hereafter OLO12, spans ~1084 ± 4 ka to 83 ± 3 ka and is remarkably well dated with 22 $^{40}Ar/^{39}Ar$ dates (average 1σ error = 5.7 kyr) and the Brunhes-Matuyama paleomagnetic reversal (Deino et al., 2019). The stratigraphy of the core allows for direct correlation to the outcrop record, providing further age constraint on sediment and hominin assemblage data (Potts et al., 2020). Initial paleoenvironmental reconstructions from OLO12 document a shift in resource base at ~470 ka potentially caused by an increase in tectonic activity and associated basin compartmentalization and enhanced topographic relief, leading to higher lake-level and vegetation variability starting at 400 ka (Potts et al., 2020).

1.2. Evolutionary hypotheses

There are many hypotheses linking environmental change to hominin evolution. The 'savanna hypothesis' is one of the earliest of these and posited an impact of gradual reductions in tree cover and grassland emergence on the anatomy and behavior of our early human ancestors (Dart, 1925). More recent hypotheses proposed linkages between the rate of environmental change and/or environmental variability and human evolution. The 'turnover pulse hypothesis' proposes that rapid, directional changes in habitat, caused by climate or tectonic events, drive a range of evolutionary responses by hominins and other large mammals on the landscape (Vrba, 1985, 1993). This hypothesis would be supported by observations of a correlation between singular climatic shifts or events and widespread evolutionary change. The 'variability selection hypothesis' posits that climate and environmental variability, rather than unidirectional shifts or events, creates selective pressure for more generalist traits (Potts, 1996; Potts and Faith, 2015). The emergence of high-resolution, quantitative proxy records indicates that time intervals of high-amplitude climatic and environmental variability may correspond with intervals of hominin evolutionary change (e.g., Trauth et al., 2007; Lupien et al., 2018) in support of this hypothesis, but there is a still a lack of long, high-resolution, environmental records from hominin fossil locales,

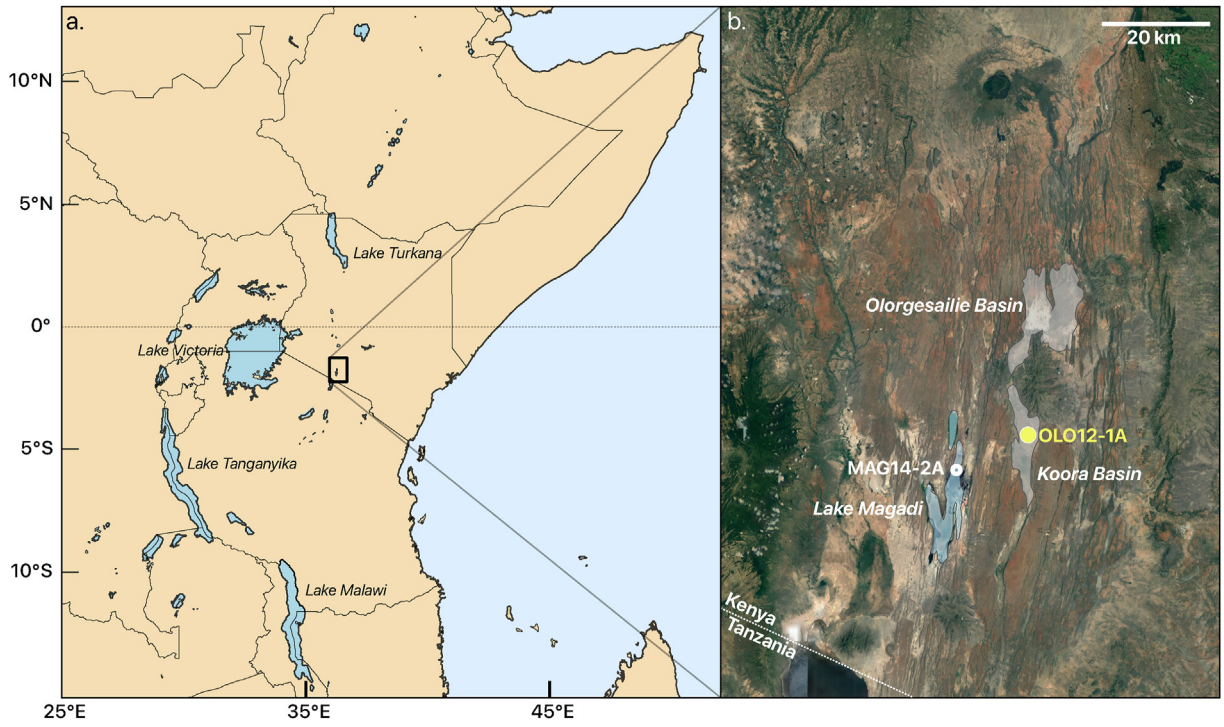

Figure 1. (a) Eastern African study area and (b) regional Google Earth image indicating the Olorgesailie Basin, the downstream Koora Basin containing OLO12 drill site, and the nearby Lake Magadi with drill core MAG14-2A in the southern Kenya rift.

and thus, the climate and environmental impact on early humans remains unclear.

Here, we examine stable carbon isotope ratios of plant wax biomarkers ($\delta^{13}C_{wax}$) to identify basin-scale C_3–C_4 vegetation variability from ~1 Ma to ~90 ka in the Koora-Olorgesailie region and $\delta^{13}C$ from bulk organic matter ($\delta^{13}C_{OM}$), which provides a continuous high-resolution (orbital-scale) record of ecosystem fluctuations throughout this time and allows us to test these various evolutionary hypotheses. The plant wax and OM carbon isotope reconstructions presented in Potts et al. (2020) have relatively low temporal resolution and contain gaps, whereas the new records presented here provide the resolution to reconstruct orbital-scale cycles and long-term trends needed to evaluate high- and low-latitude influences on the local environment.

2. Materials and methods

Epicuticular waxes are produced by plants to reduce evaporation and physical damage (Eglinton and Hamilton, 1967). These waxes are ablated from plant surfaces, transported from the catchment, deposited in sedimentary archives, and preserved over geological time. Terrestrial plant waxes are composed of long-chain hydrocarbons (Eglinton and Hamilton, 1967; Volkman et al., 1998; Sachse et al., 2012), including *n*-alkanoic acids or 'fatty acids', which we analyzed for their carbon isotopic composition in samples from the OLO12 drill core. Plants with different metabolic pathways (C_3 and C_4) fractionate carbon differently during photosynthesis (O'Leary, 1981), and thus the carbon isotopic composition of the waxes ($\delta^{13}C_{wax}$) can indicate plant type. In eastern Africa, C_3 plants are dominantly woody dicots (trees and shrubs), whereas C_4 plants are dominantly grasses (Tieszen et al., 1979; Cerling and Harris, 1999). The relative abundance of trees versus grasses is strongly influenced by precipitation because of a variety of physiological differences related to water stress, although vegetation can also be influenced by rainfall seasonality, growing season temperature, pCO_2, herbivory, and fire (Sankaran et al., 2005; Bond, 2008; Asner et al., 2009; Lehmann et al., 2014; Ivory et al., 2018; Dupont et al., 2019). $\delta^{13}C_{wax}$ records from paleolake sediment have documented that eastern African vegetation fluctuates throughout the entire C_3–C_4 spectrum on orbital timescales (e.g., Magill et al., 2013; Colcord et al., 2018; Lupien et al., 2018, 2021).

For plant wax isotope analysis, we sampled 59 sediment aliquots from undisturbed faces of the split OLO12 core, stored at the National Lacustrine Core Facility (LacCore). The samples integrate on average 6 cm of core depth (maximum 17 cm) or 558 years. Lipids from freeze-dried sediment were extracted with dichloromethane:methanol (9:1) using a DIONEX Accelerated Solvent Extractor 350. The lipids were split into neutral and acid fractions over an aminopropylsilyl gel column with dichloromethane:isopropanol (2:1) and ether:acetic acid (24:1) as eluents, respectively. The acid fractions were methylated with acidified methanol at 60 °C overnight to produce fatty acid methyl esters (FAMEs), which were purified via silica gel column chromatography with hexane and dichloromethane as eluents. Compound-specific FAMEs concentrations were quantified using an Agilent 6890 gas chromatograph (GC) equipped with an HP1-MS column (30 m × 0.25 mm × 0.25 μm) and flame ionization detector. Distributions were summarized using the average chain length (ACL; as in Castañeda et al., 2016) and the Carbon Preference Index (CPI; Bray and Evans, 1961), which quantifies the odd to even chain length preference to measure the degradation of the waxes, where petroleum sources have CPI values of 1, and higher plants have CPI values above 3. Carbon isotopes of waxes ($\delta^{13}C_{wax}$) were analyzed on an Agilent 6890 GC equipped with HP1-MS column (30 m × 0.25 mm × 0.10 μm) coupled to a Thermo Delta V Plus isotope ratio mass spectrometer (IRMS; combustion reactor at 1100 °C) at Brown University. Samples were measured in duplicate with an average intrasample difference of 0.24‰. The IRMS was run with three pulses of CO_2

reference gas standard before and after each injection and a FAMEs laboratory standard with five FAMEs of known isotopic composition (ranging from −26.8 to −30.1‰; n-C_{28} = −27.6‰ was measured every seventh injection). This 'in-house' standard mix was used to monitor instrument performance and correct for drift, if needed. These standards yielded a standard deviation (1σ) of 0.24‰. In-house standards were calibrated against a mixture of C_{20} fatty acid ester Schimmelmann standards. All sample measurements were corrected for the isotopic composition of the added methyl group during methylation, where $\delta^{13}C_{MeOH}$ = −36.52‰. Sixty percent of these $\delta^{13}C_{wax}$ data are reported in Potts et al. (2020).

To infer the relative abundance of C_3 and C_4 vegetation from $\delta^{13}C_{wax}$ (Fig. 2), we use eastern African n-C_{30} fatty acid values of −32.9‰ for C_3 and −19.0‰ for C_4 based on Uno et al. (2016b). Because isotope homologs n-C_{30} and n-C_{28} used in this study show negligible offset (Chikaraishi et al., 2004), including in this region (Uno et al., 2016b), we use these endmember values to infer 100% and 0% C_3 plants, respectively. C_3 plants can have more negative $\delta^{13}C_{wax}$ values than this chosen endmember (Vogts et al., 2009); yet, these ^{13}C-depleted closed canopy forest plant types are likely unsubstantial on this landscape, as demonstrated by the multiproxy data in Potts et al. (2020). Crassulacean acid metabolism plants, which have intermediate $\delta^{13}C_{wax}$ values, are also unlikely to be present in high enough concentrations in this region (Potts et al., 2020) to necessitate inclusion in a mixing model (Cerling, 2014). Furthermore, proximal or submerged C_4 plants could influence the measured isotope value (Liu et al., 2015) but would have minimal effect because of the spatial and temporal integration in our measurements. Our interpretation of the $\delta^{13}C_{wax}$ record is further supported by phytolith-based records of the abundance of tree and grass cover (Supplementary Online Material [SOM] S1; SOM Fig. S1).

Our ability to measure $\delta^{13}C_{wax}$ in OLO12 was ultimately limited by low plant wax concentrations. In addition to $\delta^{13}C_{wax}$, we analyzed the carbon isotopic composition of bulk sedimentary $\delta^{13}C_{OM}$ to provide a more continuous indicator of ecosystem change. Lake sediment preserves bulk OM from both aquatic and terrestrial sources, and thus, $\delta^{13}C_{OM}$ records both aquatic carbon cycling and terrestrial C_3/C_4 plant abundance (Meyers and Teranes, 2002). C_3 vascular plants (i.e., trees and shrubs) and phytoplankton (i.e., C_3 algae) have similar carbon isotopic values when algae use dissolved CO_2 as a carbon source for photosynthesis, making these sources difficult to differentiate. $\delta^{13}C_{OM}$ can become more ^{13}C-enriched through the input of C_4 plants and through OM input derived from phytoplankton that either metabolize bicarbonate (HCO_3^-), which occurs when CO_2 is limited and alkalinity is high (Hassan et al., 1997; Meyers and Teranes, 2002), or a dissolved inorganic carbon source enriched in ^{13}C because of recycling in a closed-basin lake environment with a long residence time (e.g., Hollander and McKenzie, 1991; Bernasconi et al., 1997; Talbot et al., 2006). Eastern African lacustrine $\delta^{13}C_{OM}$ has been shown to track changes in terrestrial plant type, likely through a combination of the processes described previously and inputs of terrestrial dissolved organic carbon that are subsequently used by phytoplankton (Russell et al., 2009; Webb et al., 2016). In nearby Lake Turkana, Lupien et al. (2018) recorded a significant correlation (r = 0.43, p < 0.0001, n = 168) between $\delta^{13}C_{OM}$ and $\delta^{13}C_{wax}$. Thus, positive $\delta^{13}C_{OM}$ values commonly signify an arid (low lake level) lacustrine and/or the abundance of grasslands within the lake catchment, which often co-occur in this region.

A total of 294 samples was analyzed for $\delta^{13}C_{OM}$. Samples were acidified in 2N hydrochloric acid (HCl) for 1 hour at 80 °C to remove carbonate minerals, rinsed in deionized water and centrifuged four times to remove excess HCl, and then lyophilized and homogenized before isotopic analysis. $\delta^{13}C_{OM}$ values were measured with a Carlo Erba Elemental Analyzer coupled to a Thermo Delta Plus IRMS. The analytical precision determined through replicate measurements of internal sediment standards was 0.14‰. We report $\delta^{13}C$ from wax and bulk OM in per mil (‰) relative to Vienna PeeDee Belemnite. Forty percent of these $\delta^{13}C_{OM}$ data was reported previously in Potts et al. (2020); our new dataset substantially increases the temporal resolution of this record.

We calculated the Pearson correlation coefficient between $\delta^{13}C_{OM}$ and $\delta^{13}C_{wax}$ in the OLO12 drill core using the closest $\delta^{13}C_{OM}$ measurement within 10 cm of a $\delta^{13}C_{wax}$ measurement (SOM S1). The time series of $\delta^{13}C_{OM}$ was analyzed for patterns and significance of shifts in trend, variance, and periodicity using Excel v.16.48 and the Signal Processing Toolbox in MATLAB (MathWorks, 2020). Lomb–Scargle spectral analysis of nonuniformly sampled data with the 'plomb' function was performed conservatively on the interval with highest resolution (no more than 10 kyr between datapoints, mean of 2.3 kyr between datapoints), which spans over 300 kyr from ~485 ka to 165 ka (SOM S1). This interval captures high and low eccentricity, as well as glacial and interglacial periods; thus, we assume this truncated window to be unbiased in capturing boundary conditions. The higher data resolution in this interval is

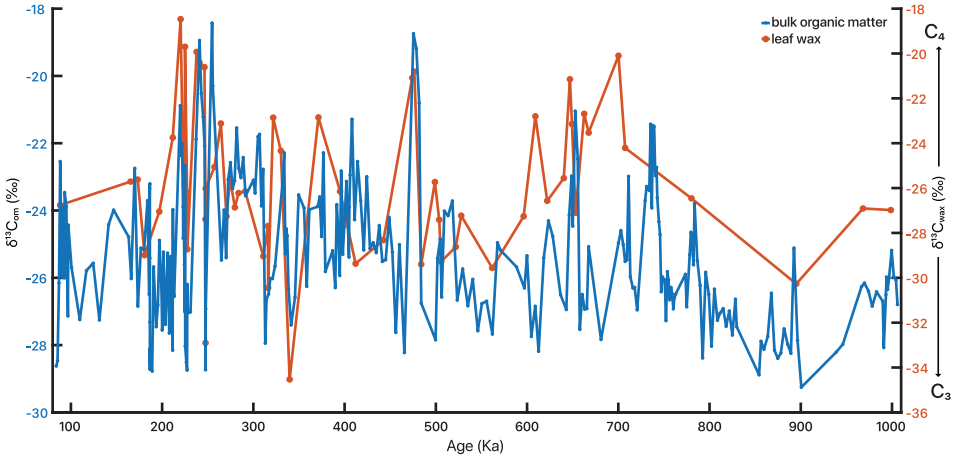

Figure 2. Bulk organic matter carbon isotope record ($\delta^{13}C_{OM}$) in blue (y-axis on the left) and plant wax carbon isotope record ($\delta^{13}C_{wax}$) in orange (y-axis on the right). The two organic carbon isotope records demonstrate general covariation as well as high-amplitude fluctuations in landscape and environment over the last 1 Myr. (For interpretation of the references to color in this figure legend, the reader is referred to the Web version of this article.)

because of the increase of sedimentation rate at ~400 ka, likely caused by enhanced volcano–tectonic activity in the region, which also results in better age constraint in this upper portion of OLO12 (Deino et al., 2019; Potts et al., 2020). We plot the spectral properties (SOM Fig. S2) between the frequencies of the Nyquist and 1/3 of the total study interval.

To investigate trends and variance in $\delta^{13}C_{OM}$ in OLO12, we resampled the ~900 kyr-long record to 10 kyr resolution to minimize data density biases (SOM S1; SOM Fig. S3). The moving variance was characterized using 7-, 9-, and 11-datapoint windows (70, 90, and 110 kyr, respectively); the effect of varying window size did not change results. Trends in variance were extracted by fitting a linear regression to the moving variance curve. The MATLAB 'findchangepts' tool identified changepoints or robust shifts in standard deviation and mean through time. This function creates a stepwise model with a cost penalty for each additional changepoint to most effectively reduce the residual mean-squared error to find the optimal timing and number of changepoints. To extract a robust signal of long-term shifts, we applied a minimum threshold constraint of the dataset's root mean-squared error for both mean and variance changepoint analyses. The significance of the timing and abruptness of the shift in mean were analyzed with a running Mann–Whitney U-test for central tendency (Mann and Whitney, 1947) using the MATLAB 'ranksum' function and windows of 10, 20, and 30 datapoints.

3. Results

We observe strong and significant correlations among the carbon isotopic values of long-chain *n*-acids ($r_{C26\text{-}C28} = 0.87$, $p_{C26\text{-}C28} < 0.0001$, $n = 59$; $r_{C28\text{-}C30} = 0.89$, $p_{C28\text{-}C30} < 0.0001$, $n = 57$), which suggests the plant wax isotope homologs in the samples are derived from a common source, likely vascular plants (Sachse et al., 2012). Long-chain wax homolog distributions in OLO12 are consistently dominated by *n*-C_{28}, and in light of the positive correlations among homologs, we use *n*-C_{28} to represent the $\delta^{13}C_{wax}$ analyses. The ACL of long-chain alkanoic acid compounds (*n*-C_{26} to *n*-C_{32}) is 28.4, and average OLO12 CPI is 3.5, with a minimum of 1.9. CPI and $\delta^{13}C_{wax}$ are significantly correlated ($r = 0.74$, $p < 0.0001$, $n = 59$), yet degradation is not thought to strongly influence $\delta^{13}C_{wax}$ (Huang et al., 1997; Nguyen Tu et al., 2004); this correlation can arise from environmental processes that affect both plant wax degradation and isotopic composition. For instance, aridification is linked to low lake levels, which can result in decomposition of the waxes because of exposure to oxidative conditions and thus a lower CPI value, and aridification can also favor C_4 grassland expansion and thus ^{13}C-enriched $\delta^{13}C_{wax}$. OLO12 $\delta^{13}C_{wax}$ has a mean of −25.7‰ and ranges between −34.5‰ and −18.5‰ (Fig. 2). Our record documents a long-term average of equally mixed C_3/C_4 plants over the last 1 Myr, and the data span the entire range of vegetation type between the C_3 and C_4 endmembers (Fig. 2), similar to other long, orbitally resolved $\delta^{13}C_{wax}$ records from eastern African lakes (e.g., Johnson et al., 2016; Lupien et al., 2018, 2021).

The $\delta^{13}C_{OM}$ averages −25.3‰ and varies between −29.2‰ and −18.4‰ (Fig. 2). The similarity in means between the two carbon records, despite a systematic offset in the nearby Oldupai Gorge (Magill et al., 2013), is likely due to the difference in sample distribution of the two carbon records throughout the OLO12 core. The relative ^{13}C enrichment of the most negative $\delta^{13}C_{OM}$ values relative to the most negative $\delta^{13}C_{wax}$ values could result from the addition of ^{13}C-enriched aquatic OM into the bulk sedimentary OM (Meyers and Teranes, 2002) or the relative ^{13}C depletion of waxes compared with bulk tissue of terrestrial plants (Collister et al., 1994; Magill et al., 2013). The correlation between $\delta^{13}C_{wax}$ and $\delta^{13}C_{OM}$ is relatively weak, although significant ($r = 0.52$, $p = 0.0038$, $n = 29$), and the two are more closely correlated after 400 ka ($r = 0.69$, $p = 0.0063$, $n = 14$; SOM S1; SOM Fig. S4), where the data density is high (Deino et al., 2019; Potts et al., 2020). There is negligible effect of lithology on $\delta^{13}C_{OM}$ (SOM S1; Fig. 3). Based on the correlations between $\delta^{13}C_{wax}$ and $\delta^{13}C_{OM}$, the significant relationship of $\delta^{13}C_{wax}$ with the phytolith tree cover index (SOM Fig. S1) and the effects of lake level on $\delta^{13}C_{OM}$, we interpret OLO12 $\delta^{13}C_{OM}$ as a general indicator of climate and environment, incorporating signals of lake level and terrestrial vegetation, wherein more positive $\delta^{13}C_{OM}$ values signify a drier climate, expanded grasslands, and/or lower lake levels.

After resampling the $\delta^{13}C_{OM}$ record at a 10 kyr-year step, we observe a linear trend toward more positive values in $\delta^{13}C_{OM}$ ($r = -0.54$, $p < 0.0001$, $n = 93$). This trend is marked by a shift identified in our changepoint analysis at ~790 ka that more significantly reduces the residual error (Fig. 4b). The significance of the timing of this shift is also highlighted by the running Mann–Whitney test, which consistently documents this single change across window sizes (Fig. 4c). The evenly resampled $\delta^{13}C_{OM}$ also exhibits discrete packets of high variability, particularly from ~275 ka to ~180 ka (Fig. 4d), which is also an interval of considerable variability in $\delta^{13}C_{wax}$. $\delta^{13}C_{OM}$ increases in variance through time ($r = -0.34$, $p = 0.0009$, $n = 93$; Fig. 4d) and changepoint analysis suggests an increase in variance at ~790 ka (Fig. 4b), similar to the shift in mean $\delta^{13}C_{OM}$.

Lomb–Scargle spectral analysis of the 485–165 ka interval of $\delta^{13}C_{OM}$, during which sampling resolution is appropriately and consistently high enough for the application of spectral analyses, documents significant periodicities at 23 kyr and at 123 kyr (SOM Fig. S2), although the low-frequency result should be interpreted with caution because of its spectral position near half the length of the study interval. We also find spectrally dense bands at 19 kyr and 12–13 kyr (SOM Fig. S2).

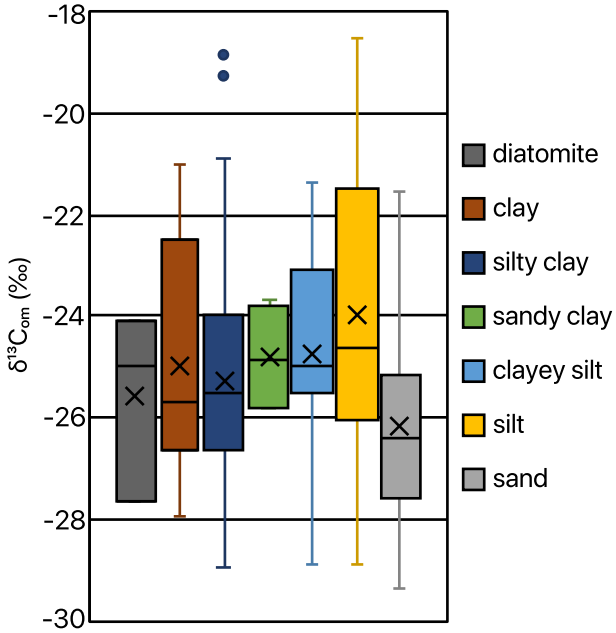

Figure 3. Box and whisker plots of $\delta^{13}C_{OM}$ grouped by sediment type in OLO12 demonstrate little effect from lithology on carbon isotope values. The mean is indicated by the '×', upper and lower quartiles with whiskers, middle two quartiles in the box separated by the median (horizontal) line, and outliers as dots.

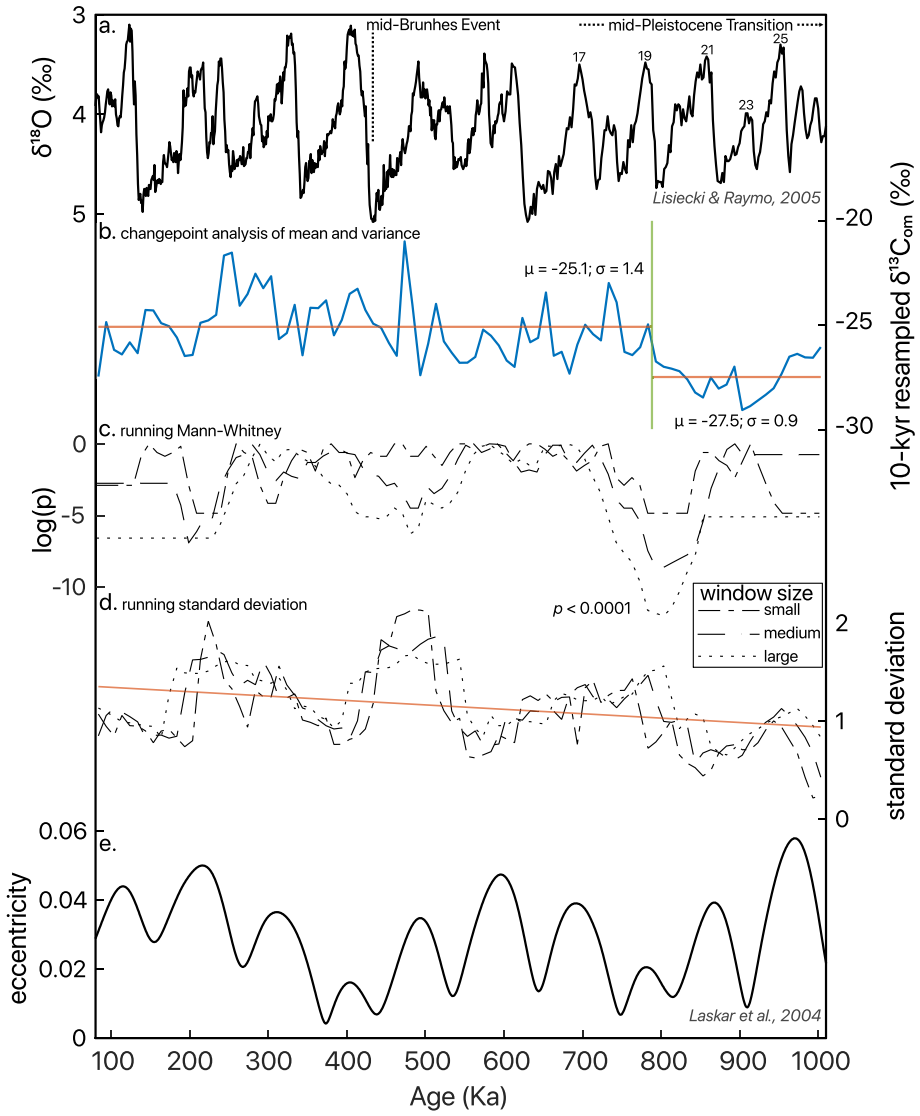

Figure 4. (a) Time series analyses of the 10-kyr resampled bulk organic matter carbon isotope record ($\delta^{13}C_{OM}$) compared with the benthic foraminifera oxygen isotope stack with marine isotope stages during the mid-Pleistocene transition noted (Lisiecki and Raymo, 2005); (b) Changepoint analysis of mean (μ) and standard deviation (σ) document a significant shift toward aridification and increased variability at ~790 ka; (c) A running Mann–Whitney U-test of significance of shift in median $\delta^{13}C_{OM}$ documents a robust change ~790 ka using three window sizes (7-, 9-, and 11-point windows in dashed lines. (d) A running standard deviation test using three window sizes (10-, 20-, and 30-point windows in dashed lines) exhibits packets of high variability that generally correspond to (e) orbital eccentricity (Laskar et al., 2004), superimposed on the linear trend of increasing variability through time.

4. Discussion

Vegetation reconstructions based on the carbon isotopic composition of pedogenic carbonates (Cerling and Hay, 1986; Wynn, 2000, 2004; Levin et al., 2004, 2011; Quinn et al., 2007; Cerling et al., 2011; Levin, 2015; Quinn and Lepre, 2020), fossil teeth (Uno et al., 2011; Cerling et al., 2015), plant waxes in marine sediment (e.g., Feakins et al., 2013; Uno et al., 2016a; Polissar et al., 2019), and pollen assemblages (e.g., Bonnefille, 2010; Hoetzel et al., 2013) indicate a gradual expansion of C_4 grasslands in Africa beginning during the late Neogene and continuing in the Quaternary. Reconstructions of vegetation that are able to resolve orbital-scale cycles have generally demonstrated precession-driven climate oscillations in eastern Africa (Magill et al., 2013; Rose et al., 2016; Colcord et al., 2018; Lupien et al., 2021), albeit over shorter time intervals than the span of soil carbonate records. Some of these higher-resolution records are also long enough to document discrete packets of high-amplitude variability that coincide with the eccentricity modulation of precession (Lupien et al., 2018). However, vegetation records from eastern African lake basins that span the mid- to late-Pleistocene exhibit an array of basin-scale environmental trajectories, including progressive aridification (Owen et al., 2018; Fig. 5b) and even trends toward wetter environments (Johnson et al., 2016; Fig. 5c). Indeed, recently published multiproxy compilations from the Magadi Basin (Owen et al., 2018) and Koora Basin (Potts et al., 2020) disagree on the trajectory of environmental change despite being less than 20 km apart (Fig. 1b). Owen et al. (2018) infer a progressive drying beginning ~575 ka, whereas Potts et al. (2020) infer an increase in environmental variability after ~400 ka with little shift in long-term trend. However, both datasets suggest that orbitally driven insolation changes played a limited role in driving regional vegetation shifts relative to

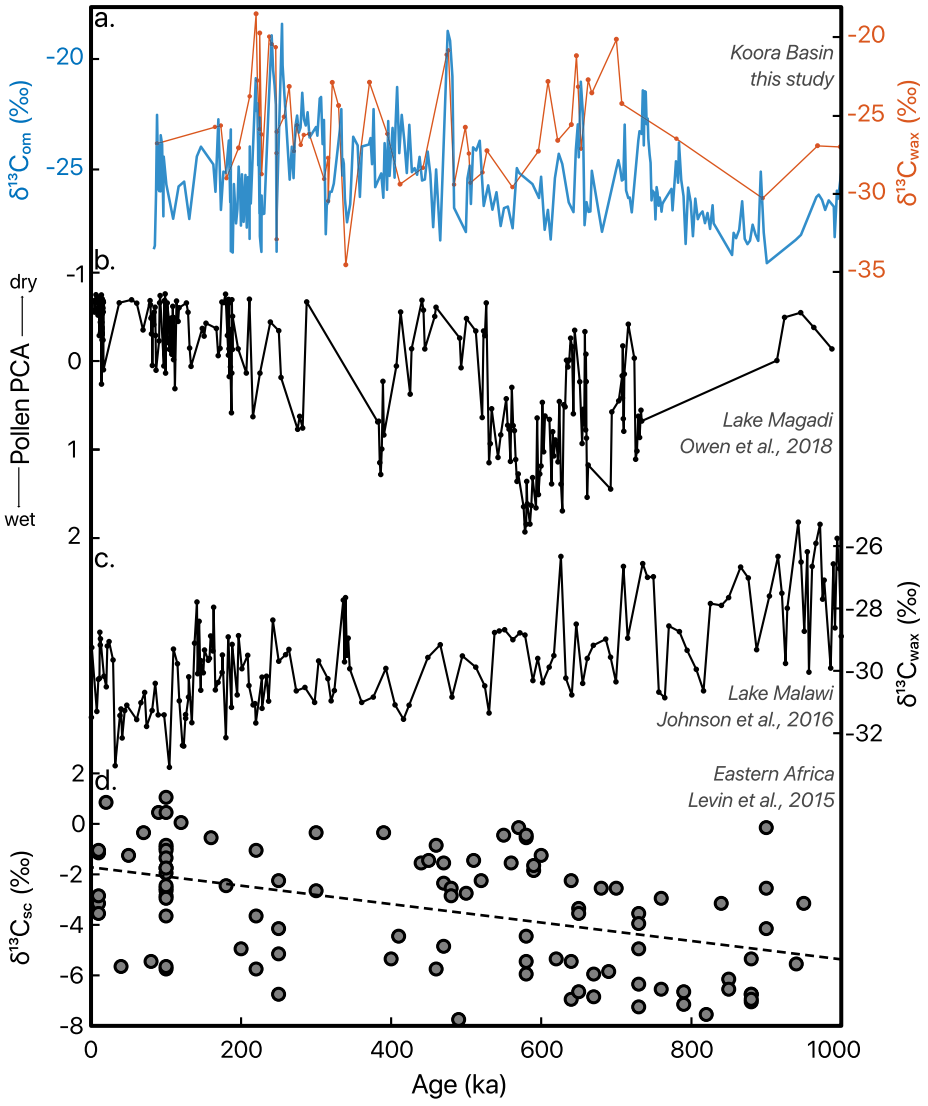

Figure 5. Carbon isotope and pollen records from eastern Africa that span the last 1 Myr demonstrate long-term changes in trend and variance. (a) The $\delta^{13}C_{OM}$ (left, blue) and $\delta^{13}C_{wax}$ (right, orange) from this study compared with the (b) wet/dry first principal component from Lake Magadi (MAG14-2A) pollen (Owen et al., 2018); (c) $\delta^{13}C_{wax}$ from Lake Malawi (Johnson et al., 2016) and (d) $\delta^{13}C_{SC}$ across multiple eastern African basins, which documents a gradual C_4 expansion, denoted by linear regression (Levin, 2015 and references therein). PCA = principal component analysis. (For interpretation of the references to color in this figure legend, the reader is referred to the Web version of this article.)

either global climate or basin geometry, despite the dominant effect of seasonal insolation forcing on the African monsoon and paleoenvironments documented in other records (e.g., Feakins et al., 2007; Tierney et al., 2017; Lupien et al., 2018).

Potts et al. (2020) infer an increase in environmental variance in OLO12 diatom, XRF, XRD, phytolith, paleosol, electrical conductivity, and initial $\delta^{13}C_{wax}$ and $\delta^{13}C_{OM}$ indicators, which capture different spatial and temporal scales and processes of environmental change. The phytolith indices of woody cover and tall versus short C_4 grasses, through time and especially from 330 ka to 220 ka (Fig. 6c and d), demonstrate an increase in vegetation variability, complemented by the increase in the frequency of soil formation periods that interrupted lacustrine phases of the Koora Basin (Fig. 6a). The authors conclude that at ~400 ka, there was a change in variance (i.e., greater instability) of vegetation and freshwater availability, likely caused by a combination of tectonic, hydrological, and ecological changes. Our new record builds on this study using high-resolution geochemical datasets spanning the entirety of the OLO12 core from 1 Ma to 90 ka. This increased resolution and more detailed comparisons between landscape proxies reflecting varying spatial and temporal scales (organics, phytoliths, and paleosols) also allow us to better understand the timing and amplitude of change, and thus, better constrain the potential impacts on hominins in the Olorgesailie Basin throughout the past 1 Myr.

4.1. Orbital insolation influences on eastern African environmental fluctuation

The seasonal distribution and intensity of solar insolation contribute to land–sea temperature and pressure gradients, which in turn control monsoonal wind and rainfall. The East African Monsoon system is thought to have strengthened and weakened with the redistribution of insolation caused by precession and amplified by eccentricity (Kutzbach et al., 2020). Reconstructions of hydroclimate (Joordens et al., 2011; Colcord et al., 2018; Lupien et al., 2018, 2021) and lake level (Kingston et al., 2007; Trauth et al., 2009; Nutz et al., 2017; Westover et al., 2021) in eastern Africa commonly exhibit orbital precession (~21 kyr) and eccentricity

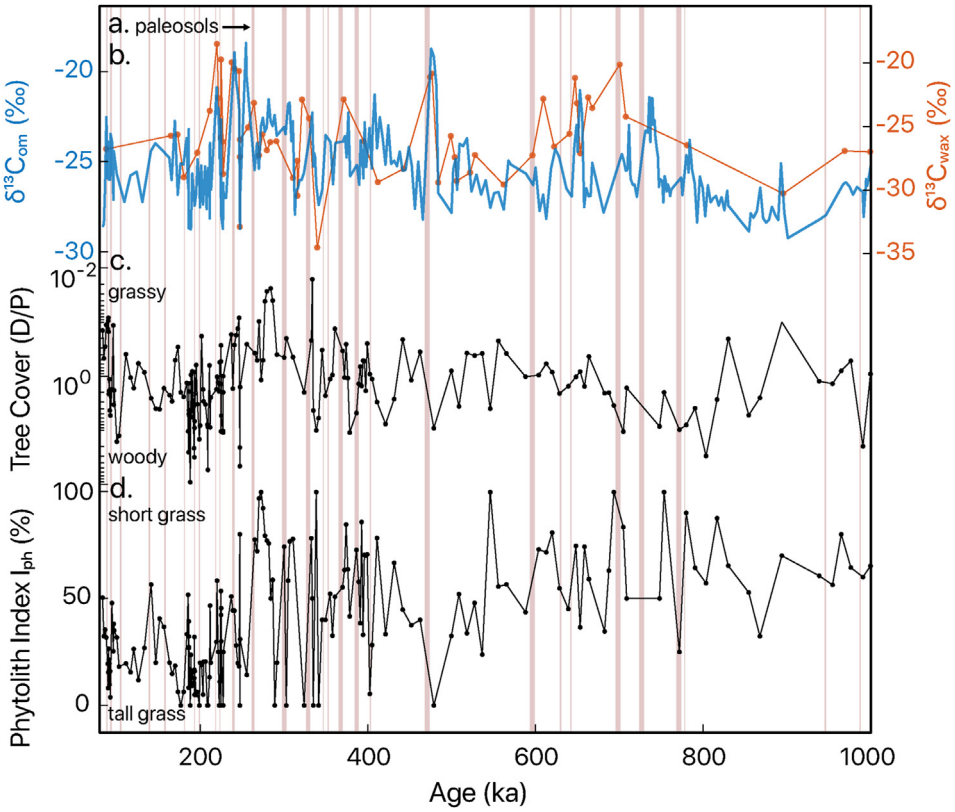

Figure 6. $\delta^{13}C_{wax}$ and $\delta^{13}C_{OM}$ records from this study (b), along with other terrestrial environment records of the Koora Basin from the OLO12 sediment core published in Potts et al. (2020) show an increase in ecosystem variance, including (a) paleosols in pink, (c) phytolith-derived indices of tree cover (D/P; Alexandre et al., 1997; Bremond et al., 2008), and (d) average grass height. (For interpretation of the references to color in this figure legend, the reader is referred to the Web version of this article.)

(~100 kyr and ~400 kyr) cycles that highlight the importance of seasonal insolation to regional hydroclimate. Precession-band variability of terrestrial vegetation has been documented in the Omo-Turkana (Lupien et al., 2018; Yost et al., in review), Baringo (Lupien et al., 2021), and Oldupai (Magill et al., 2013; Colcord et al., 2018) Basins, as well as in offshore records (Dupont, 2011; Rose et al., 2016), suggesting that monsoon strength is a significant driver of ecosystem change. Although this process causes eastern African vegetation change at orbital frequencies, most of the existing high-resolution records that span hundreds of thousands of years are from the Pliocene and early Pleistocene. There are far fewer quantitative and highly resolved vegetation records from the last 1 Myr in equatorial eastern Africa, when glacial–interglacial, atmospheric CO_2, and tropical SST cycles were stronger and potentially more influential on tropical ecosystems.

We observe large oscillations in basin-scale vegetation, and although it is unlikely that large-scale regional vegetation fully reached 100% of one photosynthetic pathway at large scales (i.e., the catchment), complete C_3–C_4 oscillation is documented, nonetheless, in other eastern African records (Magill et al., 2013; Colcord et al., 2018; Lupien et al., 2018) and suggests very large environmental changes. Running standard deviation analyses (Fig. 4d) indicate patterns that roughly correspond to eccentricity variations (Fig. 4e). This supports the spectral analysis of $\delta^{13}C_{OM}$, which shows significant coherence with eccentricity and precession (SOM Fig. S2) and even identifies both the 19 kyr and 23 kyr precession cycles. Furthermore, the strong spectral density near a half-precession periodicity (~11.5 kyr) may indicate that the landscape is potentially sensitive to both the southeasterly and northeasterly monsoons (Verschuren et al., 2009). Obliquity-band (~41 kyr) frequencies are weak, as are the impacts of obliquity on tropical insolation, suggesting that low-latitude insolation is the dominant external driver of environmental fluctuation at the orbital scale, at least during the interval from 485 ka to 165 ka, consistent with other datasets in the region.

The spectra of the OLO12 $\delta^{13}C_{OM}$ record demonstrate that despite the strong glacial–interglacial cycles of the mid- to late-Pleistocene, low-latitude insolation was a very strong influence on eastern African environmental change, as has been observed in Pliocene and earlier Pleistocene records (Kingston et al., 2007; Colcord et al., 2018; Lupien et al., 2018, 2021). Although the duration over which we calculate spectral properties of Olorgesailie vegetation variability is only 320 kyr (i.e., three eccentricity cycles), the peak in spectral density near the 100-kyr band implies eccentricity modulation of precessional-scale variability. Similar packets of hydroclimate variability are found in various hydroclimate and lake-level records (deMenocal, 2004; Trauth et al., 2007; Potts, 2013; Potts and Faith, 2015; Lupien et al., 2018) and may document the direct influence of eccentricity on insolation-forced monsoon changes. However, our new records of vegetation and ecosystem change also suggest that high-latitude-driven processes and tectonics influenced regional eastern African environments during the last 1 Myr.

4.2. Glacial–interglacial influences on eastern African environmental change

The Quaternary is characterized by large swings in glacial and interglacial climate that have far-reaching effects on the global climate system. Although lake and sapropel records provide evidence for the strong influence of low-latitude insolation on African hydroclimate, the influence of glacial–interglacial cycles (Lisiecki

and Raymo, 2005) on low-latitude wet–dry oscillations is less secure. Terrestrial dust records from marine drill cores appeared to show such an influence (deMenocal, 1995, 2004), but further analysis called into question whether the dust record, which could be related to variations in vegetation, soil moisture, and wind, is linked to any appreciable extent with a glacial–interglacial signal (Trauth et al., 2009; Skonieczny et al., 2019). A plant wax hydrogen isotope record (δD_{wax}) spanning the last 210 kyr from the Gulf of Aden does demonstrate, nevertheless, the influences of both glacial boundary conditions and low-latitude insolation on eastern African hydroclimate (Tierney et al., 2017). Furthermore, numerous records of African climate during and since the Last Glacial Maximum (LGM) indicate strong impacts of the LGM, Heinrich Events, and the Younger Dryas (e.g., Tierney et al., 2008, 2010; Costa et al., 2014) on eastern African climate, documenting teleconnections between high-latitude and African climate. Thus, although there is evidence of influence from both high-latitude climate and low-latitude insolation on hydroclimate in terrestrial eastern Africa, our long record spanning the mid- to late-Pleistocene can help to clarify the relative influence of each of these factors during a time when high-latitude climate variability shifted in frequency and amplitude.

Soil carbonate records from eastern Africa document gradual Plio-Pleistocene ^{13}C enrichment (Cerling and Hay, 1986; Wynn, 2000, 2004; Levin et al., 2004, 2011; Quinn et al., 2007; Cerling et al., 2011; Quinn and Lepre, 2020, Fig. 5d) signifying C_4 expansion, but the temporal resolution of these records is low, and soil carbonates typically form in dry seasons (e.g., Breecker et al., 2009), potentially biasing these records. Owen et al. (2018) used fossil pollen data to document drying and C_4 expansion in the Magadi Basin (Fig. 5b), close to our Koora Basin (OLO12) record in the last 1 Myr, although as noted previously, this trend differs from the lack of secular change in hydroclimate inferred from previous analyses of OLO12. Johnson et al. (2016) document a prolonged trend toward increased C_3 vegetation over the last 1.5 Ma in the Malawi Basin (11°S; Fig. 5c), although this trend may be influenced by changes in the basin configuration and is not replicated in soil carbonate records (Lüdecke et al., 2016, 2018). Higher-resolution $\delta^{13}C_{wax}$ and pollen records in the Limpopo River catchment in southeastern Africa document variation consistent with ice volume and SST cycles from 800 ka to present (Castañeda et al., 2016; Caley et al., 2018; Dupont et al., 2019), in contrast to earlier records from eastern and northeastern Africa that demonstrate predominantly precessional variability in the early to mid-Pleistocene (Rose et al., 2016; Colcord et al., 2018; Lupien et al., 2018, 2021). Various other records of $\delta^{13}C_{wax}$ that span the last few thousand years also document landscape fluctuation in concert with high-latitude-driven oscillations on these finer timescales (e.g., Garcín et al., 2014).

Our ~900 kyr-long record from the Koora Basin cannot resolve all of these discrepancies, but it is sufficiently temporally resolved to capture orbital-scale variability and sufficiently long to capture shifts in ecosystem sensitivity to global or regional boundary condition changes. The weak but significant trend toward ^{13}C enrichment in bulk OM is consistent with Pleistocene records elsewhere in eastern Africa documenting C_4 plant expansion and a drying climate (Cerling and Hay, 1986; Wynn, 2000, 2004; Levin et al., 2004, 2011; Quinn et al., 2007; Cerling et al., 2011; Quinn and Lepre, 2020). Changepoint analysis detected a shift in mean $\delta^{13}C_{OM}$ at ~790 ka toward more ^{13}C-enriched values (+2.4‰) after the MPT (Mudelsee and Schulz, 1997, Fig. 4b), an interval during which ice volume and greenhouse gas concentrations also increased in amplitudes of variability (EPICA Team Members, 2004; Lisiecki and Raymo, 2005). This changepoint in $\delta^{13}C_{OM}$, specifically at MIS 20 (Fig. 4a), is supported by the running Mann–Whitney analysis, which documented a highly significant change in mean at this event in a variety of window sizes (Fig. 4c). The carbon isotopic shift appears to have been driven predominantly by a progressive increase in ^{13}C-enriched values, interpreted as intervals of expanded grassland ecosystems. The enriched values and grassland expansion also likely drove the stepwise shift toward increased variability during the MPT transition (~790 ka) and at the MBE (~430 ka). The weak covariation between the running standard deviation of $\delta^{13}C_{OM}$ (Fig. 4d) and eccentricity (Fig. 4e) indicates that this progressive increase in variance (Fig. 4b) dominates the character of landscape variability in the Koora Basin and its catchment.

Some $\delta^{13}C_{wax}$ and associated biomarker proxy records from southern sub-tropical Africa show similar vegetation changes, including the presence of environmental responses to the high-latitude climate changes during the MPT and MBE (Castañeda et al., 2016; Johnson et al., 2016). There are inconsistencies, however, in the direction of the long-term trend throughout the Pleistocene (Fig. 5c). Pollen analysis, including the counts of grass versus aquatic pollen and the pollen principal component analysis from the Magadi Basin (Owen et al., 2018; Muiruri et al., 2021), located near the Olorgesailie Basin (Fig. 1b), also exhibit an aridification response near the MBE (Fig. 5b), as does phytolith evidence of woody cover from Olorgesailie outcrops (Kinyanjui et al., 2021). Although the mechanisms behind the increased amplitude of glacial–interglacial cycles at the MBE are debated (e.g., Clark and Pollard, 1998; Tziperman and Gildor, 2003), similarities in the timing of the stepwise increase of temperature extremes in global climate records and the Koora $\delta^{13}C_{OM}$ imply the existence of a teleconnection between the high latitudes and tropical ecosystems, possibly by way of changes in the tropical rainbelt position (Lee et al., 2015), atmospheric greenhouse gases and mean air temperatures (Otto-Bliesner et al., 2014), and/or SST-driven moisture advection (Tierney et al., 2011). A cooler climate could have caused eastern Africa to experience less humid air and shallower atmospheric convection, reducing precipitation and promoting less dense vegetation and/or grassland expansion. Furthermore, the presence of larger northern hemisphere ice sheets following the MPT likely shifted the rainbelt southward during glacials (Otto-Bliesner et al., 2014), triggering aridification in equatorial Africa. A transition toward larger Eurasian ice sheets (e.g., Valla et al., 2011) and weaker thermohaline circulation (Pena and Goldstein, 2014; Hodell and Channell, 2016) during glacial periods in response to gradual cooling has been documented during the MPT and could have promoted tropical aridification and C_4 plants by way of reduction in global temperature, atmospheric CO_2 concentrations (EPICA Team Members, 2004), and southward rainbelt displacement (Lee et al., 2015) during these intervals.

Geomorphic changes, such as changes in accommodation space, basin topography, or hydrological connectivity in the Koora Basin, may have also contributed to marked increases in landscape variability during the late Quaternary and driven a change in the environmental imprint on the sediment archive. $\delta^{13}C_{wax}$ of long-chain *n*-acids, a purer tracer of terrestrial vegetation type than $\delta^{13}C_{OM}$, documents no long-term trend in mean or variance, and thus, it is possible that the ^{13}C enrichment and increased variability we find in $\delta^{13}C_{OM}$ indicate a reduction in the catchment area and thus an increase in sensitivity to external drivers because of tectonics or hydroclimate. In particular, the increase in the most positive values at ~480 ka toward higher ecosystem variance corresponds with other proxy records from OLO12 (Fig. 6), particularly the increase in the number of paleosols (Fig. 6a), which generally correspond to more ^{13}C-rich values from waxes and OM (Potts et al., 2020). These changes in the Koora Basin also correspond with proxy records from the Magadi Basin (Owen et al., 2018, Fig. 5b). Notably, there was increased volcano-tectonism in the region

around 480 ka that may indicate strong geological impacts on local environments (Behrensmeyer et al., 2018; Deino et al., 2019). However, the occurrence of these transitions in multiple basins at the time of the MBE is striking, and the earlier (and in the Koora Basin statistically more robust) landscape shift at ~790 ka does not appear to relate to local tectonic change. Thus, overall, we infer that the increase in environmental variance over the last 1 Myr, and shifts at MPT and MBE boundary condition transitions, reflect extratropical (i.e., not low-latitude mean summer insolation) effects influencing eastern African ecosystems.

4.3. Hominin evolution

Taken together, the carbon isotopic and associated lithological and paleoenvironmental data from the Olorgesailie-Koora Basins document shifts toward more open landscapes and greater landscape variability ~790 ka (near the end of the mid-Pleistocene global climate transition) and ~430 ka (the Mid-Brunhes global climate transition). Our results, which are at a higher resolution than previously published for eastern Africa, may imply that the combination of highly variable ecosystems coupled with at least two key intervals (MPT and MBE) of drier grassland expansion may also be found in other highly resolved environmental datasets from eastern Africa. Orbital-scale variability in our record (~8‰) is, however, of much greater amplitude than the secular ^{13}C enrichment in $\delta^{13}C_{OM}$ (~2.5‰), which implies that environmental variability over such time scales likely had the larger and more proximate impact on terrestrial habitats, selection, and evolution.

Our data provide new constraints on evolutionary hypotheses as they represent well dated, high-resolution analyses of sites directly adjacent to fossil localities. Although our $\delta^{13}C_{OM}$ data cannot fully constrain terrestrial processes, the new records presented here are in agreement with the OLO12 multiproxy compilation (Potts et al., 2020) that shows a rise in ecological disruptions during a period of concentrated human and faunal adaptive change. Our expanded isotope evidence thus supports the interpretation that the landscape resource base became more variable and less dependable due to environmental instability.

Our $\delta^{13}C_{OM}$ record further indicates that ecosystem responses to insolation and seasonal monsoon strength included intervals of high and low variability in the environments in which hominin populations lived. Potts and Faith (2015) hypothesized that repeated, high-amplitude ecosystem fluctuations would exert evolutionary pressure on large mammals in the region and that ~100 kyr-long intervals, or packets, of highly variable environments were associated with transitions in human evolution. Maslin and Trauth (2009) similarly recognized that 85% of hominin evolutionary transitions occurred during high orbital eccentricity that included 'deep lake' intervals. Lupien et al. (2018) also linked oscillations between extreme aridity and humidity in the early Pleistocene with enhanced evolutionary transitions. However, appearance dates and artifacts in the hominin fossil record are associated with known, large age uncertainties (the Signor-Lipps effect; Signor and Lipps, 1982), highlighting the need for more comparisons and better temporal constraints and resolution on both fossil and paleoclimate records.

A potential misunderstanding about relating evolutionary change to climate and ecological variability is that an organism's reproduction and survival are tied to Earth's orbital time scales. Orbitally driven oscillations are, however, intimately tied to seasonal variability, for example, the East African Monsoon. Such oscillations induce shifts in the timing, length, and intensity of rainy and dry seasons, thus resulting in large increases or reductions in moisture, thereby changing the local-to-regional ecological contexts that influence the selection and the consequent evolution of adaptive strategies. Orbital-scale variability is thus ultimately linked to seasonal abundance and availability of food, water, and other resources (e.g., shade, shelter) that are critical to organisms. Long-term shifts in seasonality and environment because of orbital insolation variability result in longer-term climate patterns, such as packets of high or low climate variability (deMenocal, 2004, 2011; Potts and Faith, 2015), and also in the overall direction of change to drier or wetter conditions. It is by these effects on the ecological surroundings that orbital oscillations provide a proxy for shifting seasonality, resources, and fitness conditions affecting populations over evolutionary time (Potts, 1998a; Potts and Faith, 2015).

Our $\delta^{13}C$ records from the Olorgesailie-Koora region contain an interval with exceptionally high-amplitude and sustained variability (i.e., more than a single excursion) from ~275 ka to ~180 ka. This packet, associated with high eccentricity and amplified precessional insolation cycles (Fig. 4e), corresponds with the appearance of morphological traits of *H. sapiens* in eastern African by at least ~196 ka in the Lower Omo Valley, Ethiopia (McDougall et al., 2005), suggesting a potential link between an externally driven varying resource base over a broad area of eastern Africa and the evolution of morphological traits. The earliest dispersals of modern humans beyond Africa also may have occurred in this time interval (Harvati et al., 2019), indicating that the high instability of eastern African environment may relate to population expansion to other locales. Our data are consistent with the 'variability selection hypothesis' (Potts, 1996; 1998a,b) in that this lengthy interval of high ecological resource instability is associated with high eccentricity (Potts and Faith, 2015) and the proliferation of African MSA adaptations commonly associated with early *H. sapiens* (Tryon and Faith, 2013; Blinkhorn and Grove, 2018). It is unclear, however, why high-amplitude variability packets are not apparent during each high eccentricity interval in the Olorgesailie-Koora record, as well as in the early Pleistocene of the Turkana Basin (Lupien et al., 2018). Generating more records spanning multiple eccentricity cycles, as well as records that more directly record climate, will help tackle this question.

Because of the increase in high-resolution sampling of organic carbon isotopes throughout OLO12, we provide a more temporally nuanced view of the variation in resource base that hominins experienced and show that there was an increase in environmental variability around the time that Potts et al. (2020) suggest, that is, ~400 ka but also earlier at ~790 ka. Potts et al. (2020) hypothesized that this later increase in ecological resource variability led to the demise of the Acheulean in the southern Kenya rift and its replacement by MSA adaptations, including social networks that increased survivorship by mediating resource risk in progressively unstable resource base (Brooks et al., 2018; Potts et al., 2020). A roughly concurrent turnover in the fauna included the decline of megagrazers and the emergence of traits in mammal herbivores, such as smaller body mass, mixed (browser-grazer) feeding, and water independence, which appear likely to have been advantageous in a tectonically fragmented and fluctuating landscape (Potts et al., 2018). The general agreement between OLO12 plant waxes, bulk OM, phytoliths, and paleosols (Fig. 6), which record different spatial scales, indicates that food, water availability, and habitat structure became increasingly unreliable across the basin, particularly evidenced in the $\delta^{13}C_{wax}$ record during the high-amplitude packet driven by eccentricity ~275–180 ka.

The gradual increase in environmental variance in the Olorgesailie region was likely driven by enhanced glacial–interglacial cycles and regional tectonovolcanism. The mid- to late-Pleistocene increase in variability has also been recognized in millennial-scale changes in global methane and Chinese speleothem $\delta^{18}O$ (Thirumalai et al., 2020). These high-frequency cycles were directly related to orbital-scale insolation variation, which

suggests that environmental changes on time scales pertinent to hominin evolution may have also increased in amplitude through the mid- to late-Pleistocene in eastern Africa. Lupien et al. (2020) found no inherent link between orbital cycles and millennial-scale precipitation variability but did demonstrate relatively stronger, high-frequency variability during an extremely arid (isotopically more positive) interval. Thus, the progressive ^{13}C enrichment of $\delta^{13}C_{OM}$ arid maxima in the OLO12 record may have occurred in the context of increasingly unstable environments for the hominins living in and near the Olorgesailie Basin. Furthermore, this increase in landscape instability would also have increased the likelihood for high-amplitude, abrupt ecological changes (Lupien et al., 2020), which have been emphasized in agent-based models as a dominant cause of behavioral change in hominins (Grove, 2014). Simulations of evolutionary plasticity further suggest that high-amplitude, frequent, and abrupt environmental changes are drivers of hominin behavioral changes, such as geographic relocation, dietary change, and other adaptations because of a shifting resource base (Grove, 2014).

5. Conclusions

Long, high-resolution records of ecosystem change in the Koora Basin document trends, amplitudes, and cycles of terrestrial environmental change over 10 eccentricity cycles and 900 kyr of glacial–interglacial fluctuation. We tested a range of hypotheses relating environmental trends and variance with hominin evolution and adaptation and global climate perturbations. We find that the precessional fluctuations between woodland and open grassland endmembers are stronger than the long-term trend, are bundled into packets associated with high orbital eccentricity, and increase in amplitude through the mid- to late-Pleistocene. Although the pacing of terrestrial ecosystem variation is controlled by regional monsoon intensity tied to tropical seasonal insolation, the stepwise carbon isotope shift at the MPT and the increase in variance suggest that processes related to the northern high latitudes influence terrestrial ecosystems in eastern Africa. Furthermore, the $\delta^{13}C$ maxima become more positive near the end of the MPT and at the MBE, similar to glacial cycles, thermohaline circulation, and tropical SSTs.

New $\delta^{13}C_{OM}$ and $\delta^{13}C_{wax}$ reconstructions of environment and vegetation, respectively, demonstrate that major evolutionary events, including the first evidence of traits associated with *H. sapiens* in eastern Africa, occur in the context of large landscape and resource fluctuations. The progressive increase in variance could indicate that hominins and other species experienced an increasingly unstable resource base over the last 1 Myr, culminating in the selection of generalist morphologies and traits of plasticity. It is possible that the combination of progressively extreme glacial–interglacial cycles and consistent precession-driven monsoon fluctuation could result in more frequent, pronounced, and sudden landscape alterations. With more high-resolution, quantitative records of past climate and ecosystem change from Africa, we can continue to refine our understanding of how the evolution of hominin ancestors was linked to their environment.

Declaration of competing interest

The authors declare no conflict of interest.

Acknowledgments

We wish to thank Laura Messier for laboratory assistance and the members of the Olorgesailie Drilling Project and the Hominin Sites and Paleolakes Drilling Project for insightful discussions. We would also like to thank the editors and reviewers Sarah Feakins, Robert Patalano, and an anonymous reviewer for their thorough and constructive feedback toward improving the article. We acknowledge the National Museums of Kenya, the Oldonyo Nyokie Group Ranch, and the Olorgesailie field team led by J.M. Nume and J.N. Mativo. Research and drilling permits were provided by the Kenyan National Council for Science and Technology, the Kenya Ministry of Petroleum and Mining, and the National Environmental Management Authority of Kenya and facilitated by the cooperative agreement between the National Museums of Kenya and Smithsonian Institution. We thank DOSECC Exploration Services for drilling supervision, Drilling and Prospecting International for drilling services, and the LacCore and CSDCO (University of Minnesota) for initial core processing and sampling. This work was supported by the Peter Buck Fund for Human Origins Research to the Smithsonian; the William H. Donner Foundation to R.P.; the Ruth and Vernon Taylor Foundation to R.P.; and the National Science Foundation (grant number EAR 1826938) to J.M.R.

Supplementary Online Material

Supplementary online material to this article can be found online at https://doi.org/10.1016/j.jhevol.2021.103028.

References

Alexandre, A., Meunier, J.-D., Colin, F., Koud, J.-M., 1997. Plant impact on the biogeochemical cycle of silicon and related weathering processes. Geochem. Cosmochim. Acta 61, 677–682.
Asner, G.P., Levick, S.R., Kennedy-Bowdoin, T., Knapp, D.E., Emerson, R., Jacobson, J., Colgan, M.S., Martin, R.E., 2009. Large-scale impacts of herbivores on the structural diversity of African savannas. Proc. Natl. Acad. Sci. USA 106, 4947–4952.
Behrensmeyer, A.K., Potts, R., Deino, A., 2018. The Oltulelei Formation of the southern Kenyan Rift Valley: A chronicle of rapid landscape transformation over the last 500 ky. Geol. Soc. Am. Bull. 130, 1474–1492.
Behrensmeyer, A.K., Potts, R., Deino, A., Ditchfield, P., 2002. Olorgesailie, Kenya: A million years in the life of a rift basin. Soc. Sedimen. Geol. 73, 97–106.
Bernasconi, S.M., Barbieri, A., Simona, M., 1997. Carbon and nitrogen isotope variations in sedimenting organic matter in Lake Lugano. Limnol. Oceanogr. 42, 1755–1765.
Blinkhorn, J., Grove, M., 2018. The structure of the middle stone age of eastern Africa. Quat. Sci. Rev. 195, 1–20.
Bond, W.J., 2008. What limits trees in C-4 grasslands and savannas? Annu. Rev. Ecol. Evol. Syst. 39, 641–659.
Bonnefille, R., 2010. Cenozoic vegetation, climate changes and hominid evolution in tropical Africa. Global Planet. Change 72, 390–411.
Bray, E.E., Evans, E.D., 1961. Distribution of n-paraffins as a clue to recognition of source beds. Geochem. Cosmochim. Acta 22, 2–15.
Breecker, D.O., Sharp, Z.D., McFadden, L.D., 2009. Seasonal bias in the formation and stable isotopic composition of pedogenic carbonate in modern soils from central New Mexico, USA. Geol. Soc. Am. Bull. 121, 630–640.
Bremond, L., Alexandre, A., Wooller, M.J., Hély, C., Williamson, D., Schäfer, P.A., Majule, A., Guiot, J., 2008. Phytolith indices as proxies of grass subfamilies on East African tropical mountains. Global Planet. Change 61, 209–224.
Brierley, C.M., Fedorov, A.V., 2010. Relative importance of meridional and zonal sea surface temperature gradients for the onset of the ice ages and Pliocene-Pleistocene climate evolution. Paleoceanogr. Paleoclimatol. 25 https://doi.org/10.1029/2009PA001809.
Broccoli, A.J., Dahl, K.A., Stouffer, R.J., 2006. Response of the ITCZ to northern hemisphere cooling. Geophys. Res. Lett. 33.
Brooks, A.S., Yellen, J.E., Potts, R., Behrensmeyer, A.K., Deino, A.L., Leslie, D.E., Ambrose, S.H., Ferguson, J.R., d'Errico, F., Zipkin, A.M., 2018. Long-distance stone transport and pigment use in the earliest Middle Stone Age. Science 360, 90–94.
Caley, T., Extier, T., Collins, J.A., Schefuß, E., Dupont, L.M., Malaizé, B., Rossignol, L., Souron, A., McClymont, E.L., Jimenez-Espejo, F.J., 2018. A two-million-year-long hydroclimatic context for hominin evolution in southeastern Africa. Nature 560, 76–79.
Castañeda, I.S., Caley, T., Dupont, L.M., Kim, J.-H., Malaizé, B., Schouten, S., 2016. Middle to Late Pleistocene vegetation and climate change in subtropical southern East Africa. Earth Planet Sci. Lett. 450, 306–316.
Cerling, T.E., Hay, R.L., 1986. An isotopic study of paleosol carbonates from Olduvai Gorge. Quat. Res. 25, 63–78.
Cerling, T.E., 1992. Development of grasslands and savannas in east Africa during the Neogene. Palaeogeogr. Palaeoclimatol. Palaeoecol. 97, 241–247.

Cerling, T.E., Harris, J.M., 1999. Carbon isotope fractionation between diet and bioapatite in ungulate mammals and implications for ecological and paleoecological studies. Oecologia 120, 347–363.
Cerling, T.E., Wynn, J.G., Andanje, S.A., Bird, M.I., Korir, D.K., Levin, N.E., MacE, W., MacHaria, A.N., Quade, J., Remien, C.H., 2011. Woody cover and hominin environments in the past 6-million years. Nature 476, 51–56.
Cerling, T.E., 2014. Stable isotope evidence for hominin environments in Africa. In: Holland, H.D., Turekian, K.K. (Eds.), Treatise on Geochemistry, Second Edition. Elsevier Science, pp. 157–167.
Cerling, T.E., Andanje, S.A., Blumenthal, S.A., Brown, F.H., Chritz, K.L., Harris, J.M., Hart, J.A., Kirera, F.M., Kaleme, P., Leakey, L.N., Leakey, M.G., Levin, N.E., Manthi, F.K., Passey, B.H., Uno, K.T., 2015. Dietary changes of large herbivores in the Turkana Basin, Kenya from 4 to 1 Ma. Proc. Natl. Acad. Sci. USA 112, 11467–11472.
Chikaraishi, Y., Naraoka, H., Poulson, S.R., 2004. Hydrogen and carbon isotopic fractionations of lipid biosynthesis among terrestrial (C3, C4 and CAM) and aquatic plants. Phytochemistry 65, 1369–1381.
Clark, P.U., Pollard, D., 1998. Origin of the Middle Pleistocene transition by ice sheet erosion of regolith. Paleoceanogr. Paleoclimatol. 13 https://doi.org/10.1029/97PA02660.
Clark, P.U., Archer, D., Pollard, D., Blum, J.D., Rial, J.A., Brovkin, V., Mix, A.C., Pisias, N.G., Roy, M., 2006. The middle Pleistocene transition: Characteristics, mechanisms, and implications for long-term changes in atmospheric pCO2. Quat. Sci. Rev. 25, 3150–3184.
Colcord, D.E., Shilling, A.M., Sauer, P.E., Freeman, K.H., Njau, J.K., Stanistreet, I.G., Stollhofen, H., Schick, K.D., Toth, N., Brassell, S.C., 2018. Sub-Milankovitch paleoclimatic and paleoenvironmental variability in East Africa recorded by Pleistocene lacustrine sediments from Olduvai Gorge, Tanzania. Palaeogeogr. Palaeoclimatol. Palaeoecol. 495, 284–291.
Collister, J.W., Rieley, G., Stern, B., Eglinton, G., Fry, B., 1994. Compound-specific δ13C analyses of leaf lipids from plants with differing carbon dioxide metabolisms. Org. Geochem. 21, 619–627.
Costa, K., Russell, J.M., Konecky, B.L., Lamb, H.F., 2014. Isotopic reconstruction of the African humid period and Congo air boundary migration at Lake Tana, Ethiopia. Quat. Sci. Rev. 83, 58–67.
Dart, R.A., 1925. *Australopithecus africanus*: The man-ape of South Africa. In: Garwin, L., Lincoln, T. (Eds.), A Century of Nature: Twenty-One Discoveries that Changed Science and the World. University of Chicago Press, Chicago, pp. 10–20.
Deino, A.L., Potts, R., 1990. Single-crystal 40Ar/39Ar dating of the Olorgesailie formation, southern Kenya rift. J. Geophys. Res. 95, 8453.
Deino, A.L., Behrensmeyer, A.K., Brooks, A.S., Yellen, J.E., Sharp, W.D., Potts, R., 2018. Chronology of the Acheulean to Middle Stone Age transition in eastern Africa. Science 360, 95–98.
Deino, A., Dommain, R., Keller, C.B., Potts, R., Behrensmeyer, A.K., Beverly, E.J., King, J., Heil, C.W., Stockhecke, M., Brown, E.T., 2019. Chronostratigraphic model of a high-resolution drill core record of the past million years from the Koora Basin, south Kenya Rift: Overcoming the difficulties of variable sedimentation rate and hiatuses. Quat. Sci. Rev. 215, 213–231.
deMenocal, P.B., 1995. Plio-pleistocene african climate. Science 270, 53–59.
deMenocal, P.B., 2004. African climate change and faunal evolution during the Pliocene–Pleistocene. Earth Planet Sci. Lett. 220, 3–24.
deMenocal, P.B., 2011. Climate and human evolution. Science 331, 540–542.
Dupont, L.M., 2011. Orbital scale vegetation change in Africa. Quat. Sci. Rev. 30, 3589–3602.
Dupont, L.M., Caley, T., Castañeda, I.S., 2019. Effects of atmospheric CO2 variability of the past 800kyr on the biomes of southeast Africa. Clim. Past 15, 1083–1097.
Eglinton, G., Hamilton, R.J., 1967. Leaf epicuticular waxes. Science 156, 1322–1335.
EPICA Team Members, 2004. Eight glacial cycles from an Antarctic ice core. Nature 429, 623–628.
Feakins, S.J., Eglinton, T.I., deMenocal, P.B., 2007. A comparison of biomarker records of northeast African vegetation from lacustrine and marine sediments (ca. 3.40 Ma). Org. Geochem. 38, 1607–1624.
Feakins, S.J., Levin, N.E., Liddy, H.M., Sieracki, A., Eglinton, T.I., Bonnefille, R., 2013. Northeast African vegetation change over 12 my. Geology 41, 295–298.
Garcín, Y., Schefuß, E., Schwab, V.F., Garreta, V., Gleixner, G., Vincens, A., Todou, G., Séné, O., Onana, J.-M., Achoundong, G., 2014. Reconstructing C3 and C4 vegetation cover using n-alkane carbon isotope ratios in recent lake sediments from Cameroon, Western Central Africa. Geochem. Cosmochim. Acta 142, 482–500.
Grove, M., 2014. Evolution and dispersal under climatic instability: A simple evolutionary algorithm. Adapt. Behav. 22, 235–254.
Harvati, K., Harvati, K., Röding, C., Bosman, A.M., Karakostis, F.A., Grün, R., Stringer, C., Karkanas, P., Thompson, N.C., Koutoulidis, V., Moulopoulos, L.A., Gorgoulis, V.G., Kouloukoussa, M., 2019. Apidima Cave fossils provide earliest evidence of *Homo sapiens* in Eurasia. Nature 571, 500–504.
Hassan, K.M., James, B.,S.B., Spalding, R.F., 1997. Evidence for holocene environmental change from C/N ratios, and δ13C and δ15N values in Swan Lake sediments, western Sand Hills, Nebraska. J. Paleolimnol. 18, 121–130.
Hays, J.D., Imbrie, J., Shackleton, N.J., 1976. Variations in the Earth's orbit: Pacemaker of the ice ages. Science 194, 1121–1132.
Herbert, T.D., Peterson, L.C., Lawrence, K.T., Liu, Z., 2010. Tropical ocean temperatures over the past 3.5 million years. Science 328, 1530–1534.
Hodell, D.A., Channell, J.E.T., 2016. Mode transitions in Northern Hemisphere glaciation: Co-evolution of millennial and orbital variability in Quaternary climate. Clim. Past 12, 1805–1828.
Hoetzel, S., Dupont, L.M., Schefuß, E., Rommerskirchen, F., Wefer, G., 2013. The role of fire in Miocene to Pliocene C4 grassland and ecosystem evolution. Nat. Geosci. 6, 1027–1030.
Hollander, D.J., McKenzie, J.A., 1991. CO2 control on carbon-isotope fractionation during aqueous photosynthesis: a paleo-pCO2 barometer. Geology 19, 929–932.
Huang, Y., Eglinton, G., Ineson, P., Latter, P.M., Bol, R., Harkness, D.D., 1997. Absence of carbon isotope fractionation of individual n-alkanes in a 23-year field decomposition experiment with Calluna vulgaris. Org. Geochem. 26, 497–501.
Isaac, G.L., Isaac, B., 1977. Olorgesailie: Archeaological Studies of a Middle Pleistocene Lake Basin in Kenya. University of Chicago Press, Chicago.
Ivory, S.J., Lézine, A., Vincens, A., Cohen, A.S., 2018. Waxing and waning of forests: late Quaternary biogeography of southeast Africa. Global Change Biol. 24, 2939–2951.
Jansen, J.H.F., Kuijpers, A., Troelstra, S.R., 1986. A mid-Brunhes climatic event: Long-term changes in global atmosphere and ocean circulation. Science 232, 619–622.
Johnson, T.C., Werne, J.P., Brown, E.T., Abbott, A., Berke, M., Steinman, B.A., Halbur, J., Contreras, S., Grosshuesch, S., Deino, A., 2016. A progressively wetter climate in southern East Africa over the past 1.3 million years. Nature 537, 220–224.
Joordens, J.C.A., Vonhof, H.B., Feibel, C.S., Lourens, L.J., Dupont-Nivet, G., van der Lubbe, J.H.J.L., Sier, M.J., Davies, G.R., Kroon, D., 2011. An astronomically-tuned climate framework for hominins in the Turkana Basin. Earth Planet Sci. Lett. 307, 1–8.
Kingston, J.D., 1992. Stable Isotopic Evidence for Hominin Paleoenvironments in East Africa.. Ph.D. Dissertation, Harvard University.
Kingston, J.D., Deino, A.L., Edgar, R.K., Hill, A., 2007. Astronomically forced climate change in the Kenyan Rift Valley 2.7–2.55 Ma: Implications for the evolution of early hominin ecosystems. J. Hum. Evol. 53, 487–503.
Kinyanjui, R.N., Meadows, M., Gillson, L., Bamford, M.K., Behrensmeyer, A.K., Potts, R., 2021. Reconstructing vegetation history of the Olorgesailie Basin during the Middle to Late Pleistocene Using phytolith data. In: Runge, J., Gosling, W.D., Lézine, A.-M., Scott, L. (Eds.), Quaternary Vegetation Dynamics: The African Pollen Data Base. Taylor & Francis, Boca Raton.
Kutzbach, J.E., 1981. Monsoon climate of the early Holocene: climate experiment with the earth's orbital parameters for 9000 years ago. Science 214, 59–61.
Kutzbach, J.E., Otto-Bliesner, B.L., 1982. The sensitivity of the African-Asian monsoonal climate to orbital parameter changes for 9000 years BP in a low-resolution general circulation model. J. Atmos. Sci. 39, 1177–1188.
Kutzbach, J.E., Guan, J., He, F., Cohen, A.S., Orland, I.J., Chen, G., 2020. African climate response to orbital and glacial forcing in 140,000-y simulation with implications for early modern human environments. Proc. Natl. Acad. Sci. USA 117, 2255–2264.
Laskar, J., Robutel, P., Joutel, F., Gastineau, M., Correia, A.C.M., Levrard, B., 2004. A long-term numerical solution for the insolation quantities of the Earth. Astron. Astrophys. 428, 261–285.
Lee, S.-Y., Chiang, J.C.H., Chang, P., 2015. Tropical Pacific response to continental ice sheet topography. Clim. Dynam. 44, 2429–2446.
Lehmann, C.E.R., Anderson, T.M., Sankaran, M., Higgins, S.I., Archibald, S., Hoffmann, W.A., Hanan, N.P., Williams, R.J., Fensham, R.J., Felfili, J., Hutley, L.B., Ratnam, J., San Jose, J., Montes, R., Franklin, D., Russell-Smith, J., Ryan, C.M., Durigan, G., Hiernaux, P., Haidar, R., Bowman, D.M.J.S., Bond, W.J., 2014. Savanna vegetation-fire-climate relationships differ among continents. Science 343, 548–552.
Levin, N.E., Quade, J., Simpson, S.W., Semaw, S., Rogers, M., 2004. Isotopic evidence for plio–pleistocene environmental change at Gona, Ethiopia. Earth Planet Sci. Lett. 219, 93–110.
Levin, N.E., Brown, F.H., Behrensmeyer, A.K., Bobe, R., Cerling, T.E., 2011. Paleosol carbonates from the Omo Group: Isotopic records of local and regional environmental change in East Africa. Palaeogeogr. Palaeoclimatol. Palaeoecol. 307, 75–89.
Levin, N.E., 2013. Compilation of East Africa Soil Carbonate Stable Isotope Data: Integrated Earth Data Applications. https://doi.org/10.1594/IEDA/100231.
Levin, N.E., 2015. Environment and climate of early human evolution. Annu. Rev. Earth Planet Sci. 43, 405–429.
Lisiecki, L.E., Raymo, M.E., 2005. A Pliocene-Pleistocene stack of 57 globally distributed benthic δ18O records. Paleoceanogr. Paleoclimatol. 20 https://doi.org/10.1029/2004PA001071.
Lüdecke, T., Schrenk, F., Thiemeyer, H., Kullmer, O., Bromage, T.G., Sandrock, O., Fiebig, J., Mulch, A., 2016. Persistent C3 vegetation accompanied plio-pleistocene hominin evolution in the Malawi rift (Chiwondo beds, Malawi). J. Hum. Evol. 90, 163–175.
Liu, W., Yang, H., Wang, H., An, Z., Wang, Z., Leng, Q., 2015. Carbon isotope composition of long chain leaf wax *n*-alkanes in lake sediments: A dual indicator of paleoenvironment in the Qinghai-Tibet Plateau. Org. Geochem. 83–84, 190–201.
Lüdecke, T., Kullmer, O., Wacker, U., Sandrock, O., Fiebig, J., Schrenk, F., Mulch, A., 2018. Dietary versatility of early Pleistocene hominins. Proc. Natl. Acad. Sci. USA 115, 13330–13335.
Lupien, R.L., Russell, J.M., Feibel, C.S., Beck, C.C., Castañeda, I.S., Deino, A.L., Cohen, A.S., 2018. A leaf wax biomarker record of early Pleistocene hydroclimate from West Turkana, Kenya. Quat. Sci. Rev. 186, 225–235.
Lupien, R.L., Russell, J.M., Beck, C.C., Feibel, C.S., Cohen, A.S., 2020. Impacts of abrupt and high frequency climate change on hominin evolution during the early Pleistocene in the Turkana Basin, East Africa. Quat. Sci. Rev. 245.

Lupien, R.L., Russell, J.M., Yost, C.L., Kingston, J.D., Deino, A.L., Logan, J., Schuh, A., Cohen, A.S., 2021. Vegetation change in the Baringo basin, East Africa across the onset of northern hemisphere glaciation 3.3–2.6 Ma. Palaeogeogr. Palaeoclimatol. Palaeoecol. 570, 109426.
Magill, C.R., Ashley, G.M., Freeman, K.H., 2013. Ecosystem variability and early human habitats in eastern Africa. Proc. Natl. Acad. Sci. USA 110, 1167–1174.
Mann, H.B., Whitney, D.R., 1947. On a test of whether one of two random variables is stochastically larger than the other. Ann. Math. Stat. 18, 50–60.
Maslin, M.A., Trauth, M.H., 2009. Plio-Pleistocene East African pulsed climate variability and its influence on early human evolution. In: Grine, F.E., Fleagle, J.G., Leakey, R.E. (Eds.), The First Humans – Origin and Early Evolution of the Genus *Homo*. Springer, Dordrecht, pp. 151–158.
MathWorks, 2020. MATLAB Signal Processing Toolbox: User's Guide. The MathWorks, Natick, MA.
McDougall, I., Brown, F.H., Fleagle, J.G., 2005. Stratigraphic placement and age of modern humans from Kibish, Ethiopia. Nature 433, 733–736.
Meyers, P.A., Teranes, J.L., 2002. Sediment organic matter. In: Last, W.M., Smol, J.P. (Eds.), Tracking Environmental Change Using Lake Sediments. Developments in Paleoenvironmental Research, vol. 2. Springer, Dordrecht, pp. 239–269.
Milankovitch, M., 1941. Kanon der Erdebestrahlung und seine Anwendung auf das Eiszeitenproblem. Königlich Serbische Akademie.
Mudelsee, M., Schulz, M., 1997. The Mid-Pleistocene climate transition: Onset of 100 ka cycle lags ice volume build-up by 280 ka. Earth Planet Sci. Lett. 151, 117–123.
Muiruri, V.M., Owen, R.B., Lowenstein, T.K., Renaut, R.W., Marchant, R., Rucina, S.M., Cohen, A., Deino, A.L., Sier, M.J., Luo, S., Leet, K., Campisano, C., Rabideaux, N.M., Deocampo, D., Shen, C.-C., Mbuthia, A., Davis, B.C., 2021. A million year vegetation history and paleoenvironmental record from the Lake Magadi Basin, Kenya Rift Valley. Palaeogeogr. Palaeoclimatol. Palaeoecol. 567, 110247.
Nguyen Tu, T.T., Derenne, S., Largeau, C., Bardoux, G., Mariotti, A., 2004. Diagenesis effects on specific carbon isotope composition of plant n-alkanes. Org. Geochem. 35, 317–329.
Nutz, A., Schuster, M., Boës, X., Rubino, J.-L., 2017. Orbitally-driven evolution of lake Turkana (Turkana depression, Kenya, EARS) between 1.95 and 1.72 Ma: A sequence stratigraphy perspective. J. Afr. Earth Sci. 125, 230–243.
Nutz, A., Schuster, M., 2018. Comments on: "A leaf wax biomarker record of early Pleistocene hydroclimate from West Turkana, Kenya" by Lupien et al. [Quat. Sci. Rev.. 186 (2018), 225–235]. Quat. Sci. Rev. 201, 505–507.
Olaka, L.A., Odada, E.O., Trauth, M.H., Olago, D.O., 2010. The sensitivity of East African rift lakes to climate fluctuations. J. Paleolimnol. 44, 629–644.
O'Leary, M.H., 1981. Carbon isotope fractionation in plants. Phytochemistry 20, 553–567.
Otto-Bliesner, B.L., Russell, J.M., Clark, P.U., Liu, Z., Overpeck, J.T., Konecky, B.L., Nicholson, S.E., He, F., Lu, Z., 2014. Coherent changes of southeastern equatorial and northern African rainfall during the last deglaciation. Science 346, 1223–1227.
Owen, R.B., Muiruri, V.M., Lowenstein, T.K., Renaut, R.W., Rabideaux, N., Luo, S., Deino, A.L., Sier, M.J., Dupont-Nivet, G., McNulty, E.P., 2018. Progressive aridification in East Africa over the last half million years and implications for human evolution. Proc. Natl. Acad. Sci. USA 115, 11174–11179.
Pena, L.D., Goldstein, S.L., 2014. Thermohaline circulation crisis and impacts during the mid-Pleistocene transition. Science 345, 318–322.
Petit, J.-R., Jouzel, J., Raynaud, D., Barkov, N.I., Barnola, J.-M., Basile, I., Bender, M., Chappellaz, J., Davis, M., Delaygue, G., 1999. Climate and atmospheric history of the past 420,000 years from the Vostok ice core, Antarctica. Nature 399, 429–436.
Polissar, P.J., Rose, C., Uno, K.T., Phelps, S.R., deMenocal, P.B., 2019. Synchronous rise of African C4 ecosystems 10 million years ago in the absence of aridification. Nat. Geosci. 12, 657–660.
Potts, R., 1994. Variables versus models of early Pleistocene hominid land use. J. Hum. Evol. 27, 7–24.
Potts, R., 1996. Evolution and climate variability. Science 273, 992.
Potts, R., 1998. Environmental hypotheses of hominin evolution. Am. J. Phys. Anthropol. 107, 93–136.
Potts, R., Behrensmeyer, A.K., Ditchfield, P., 1999. Paleolandscape variation and early Pleistocene hominid activities: Members 1 and 7, Olorgesailie formation, Kenya. J. Hum. Evol. 37, 747–788.
Potts, R., 2013. Hominin evolution in settings of strong environmental variability. Quat. Sci. Rev. 73, 1–13.
Potts, R., Faith, J.T., 2015. Alternating high and low climate variability: The context of natural selection and speciation in Plio-Pleistocene hominin evolution. J. Hum. Evol. 87, 5–20.
Potts, R., Behrensmeyer, A.K., Faith, J.T., Tryon, C.A., Brooks, A.S., Yellen, J.E., Deino, A.L., Kinyanjui, R., Clark, J.B., Haradon, C.M., 2018. Environmental dynamics during the onset of the middle stone age in eastern Africa. Science 360, 86–90.
Potts, R., Dommain, R., Moerman, J.W., Behrensmeyer, A.K., Deino, A.L., Beverly, E.J., Brown, E.T., Deocampo, D., Kinyanjui, R., Lupien, R.L., Owen, R.B., Rabideaux, N., Riedl, S., Russell, J.M., Stockhecke, M., deMenocal, P., Faith, J.T., Garcin, Y., Noren, A., Scott, J.J., Western, D., Bright, J., Clark, J.B., Cohern, A.S., Heil Jr., C.W., Keller, C.B., King, J., Levin, N., Brady, K., Muiruri, V., Renaut, R., Rucina, S.M., Uno, K., 2020. Increased ecological resource variability during a critical transition in hominin evolution. Sci. Adv. 6, eabc8975.
Quade, J., Levin, N.E., Semaw, S., Stout, D., Renne, P., Rogers, M., Simpson, S., 2004. Paleoenvironments of the earliest stone toolmakers, Gona, Ethiopia. Geol. Soc. Am. Bull. 116, 1529–1544.
Quinn, R.L., Lepre, C.J., Wright, J.D., Feibel, C.S., 2007. Paleogeographic variations of pedogenic carbonate δ13C values from Koobi Fora, Kenya: Implications for floral compositions of Plio-Pleistocene hominin environments. J. Hum. Evol. 53, 560–573.
Quinn, R.L., Lepre, C.J., 2020. Revisiting the pedogenic carbonate isotopes and paleoenvironmental interpretation of Kanapoi. J. Hum. Evol. 140.
Roberts, P., Stewart, B.A., 2018. Defining the 'generalist specialist' niche for Pleistocene *Homo sapiens*. Nat. Hum. Behav. 2, 542–550.
Rose, C., Polissar, P.J., Tierney, J.E., Filley, T., deMenocal, P.B., 2016. Changes in northeast African hydrology and vegetation associated with Pliocene–Pleistocene sapropel cycles. Phil. Trans. R. Soc. B 371.
Ruddiman, W.F., Raymo, M.E., Martinson, D.G., Backman, J., 1989. Pleistocene evolution: Northern hemisphere ice sheets and north atlantic ocean. Paleoceanogr. Paleoclimatol. 4, 353–412.
Russell, J.M., McCoy, S.J., Verschuren, D., Bessems, I., Huang, Y., 2009. Human impacts, climate change, and aquatic ecosystem response during the past 2000 yr at Lake Wandakara, Uganda. Quat. Res. 72, 315–324.
Sachse, D., Billault, I., Bowen, G.J., Chikaraishi, Y., Dawson, T.E., Feakins, S.J., Freeman, K.H., Magill, C.R., McInerney, F.A., Van Der Meer, M.T.J., 2012. Molecular paleohydrology: Interpreting the hydrogen-isotopic composition of lipid biomarkers from photosynthesizing organisms. Annu. Rev. Earth Planet Sci. 40, 221–249.
Sankaran, M., Hanan, N.P., Scholes, R.J., Ratnam, J., Augustine, D.J., Cade, B.S., Gignoux, J., Higgins, S.I., Le Roux, X., Ludwig, F., Ardo, J., Banyikwa, F., Bronn, A., Bucini, G., Caylor, K.K., Coughenour, M.B., Diouf, A., Ekaya, W., Feral, C.J., February, E.C., Frost, P.G.H., Hiernaux, P., Hrabar, H., Metzger, K.L., Prins, H.H.T., Ringrose, S., Sea, W., Tews, J., Worden, J., Zambatis, N., 2005. Determinants of woody cover in African savannas. Nature 438, 846–849.
Signor, P.W., Lipps, J.H., 1982. Sampling bias, gradual extinction patterns and catastrophes in the fossil record. In: silver, L.T., Schultz, P.H. (Eds.), Gelogical Implications of Impacts of Large Asteroids and Comets on the Earth. The Geological Society of America, Inc., Boulder, pp. 291–296.
Sikes, N.E., Potts, R., Behrensmeyer, A.K., 1999. Early Pleistocene habitat in Member 1 Olorgesailie based on paleosol stable isotopes. J. Hum. Evol. 37, 721–746.
Skonieczny, C., McGee, D., Winckler, G., Bory, A., Bradtmiller, L.I., Kinsley, C.W., Polissar, P.J., De Pol-Holz, R., Rossignol, L., Malaizé, B., 2019. Monsoon-driven Saharan dust variability over the past 240,000 years. Sci. Adv. 5, eaav1887.
Talbot, M.R., Jensen, N.B., Lærdal, T., Filippi, M.L., 2006. Geochemical responses to a major transgression in giant African lakes. J. Paleolimnol. 35, 467–489.
Thirumalai, K., Clemens, S.C., Partin, J.W., 2020. Methane, monsoons, and modulation of millennial-scale climate. Geophys. Res. Lett. 47, e2020GL087613.
Tierney, J.E., Russell, J.M., Huang, Y., Damsté, J.S.S., Hopmans, E.C., Cohen, A.S., 2008. Northern hemisphere controls on tropical southeast African climate during the past 60,000 years. Science 322, 252–255.
Tierney, J.E., Russell, J.M., Huang, Y., 2010. A molecular perspective on Late Quaternary climate and vegetation change in the Lake Tanganyika basin, East Africa. Quat. Sci. Rev. 29, 787–800.
Tierney, J.E., Lewis, S.C., Cook, B.I., LeGrande, A.N., Schmidt, G.A., 2011. Model, proxy and isotopic perspectives on the East african humid period. Earth Planet Sci. Lett. 307, 103–112.
Tierney, J.E., deMenocal, P.B., Zander, P.D., 2017. A climatic context for the out-of-Africa migration. Geology 45, 1023–1026.
Tieszen, L.L., Senyimba, M.M., Imbamba, S.K., Troughton, J.H., 1979. The distribution of C3 and C4 grasses and carbon isotope discrimination along an altitudinal and moisture gradient in Kenya. Oecologia 37, 337–350.
Trauth, M.H., Maslin, M.A., Deino, A.L., Strecker, M.R., Bergner, A.G.N., Dühnforth, M., 2007. High-and low-latitude forcing of Plio-Pleistocene East African climate and human evolution. J. Hum. Evol. 53, 475–486.
Trauth, M.H., Larrasoaña, J.C., Mudelsee, M., 2009. Trends, rhythms and events in Plio-Pleistocene African climate. Quat. Sci. Rev. 28, 399–411.
Tryon, C., Faith, J.T., 2013. Variability in the middle stone age of eastern Africa. Curr. Anthropol. 54, S234–S254.
Tziperman, E., Gildor, H., 2003. On the mid-Pleistocene transition to 100-kyr glacial cycles and the asymmetry between glaciation and deglaciation times. Paleoceanogr. Paleoclimatol. 18 https://doi.org/10.1029/2001pa000627.
Uno, K.T., Cerling, T.E., Harris, J.M., Kunimatsu, Y., Leakey, M.G., Nakatsukasa, M., Nakaya, H., 2011. Late Miocene to Pliocene carbon isotope record of differential diet change among East African herbivores. Proc. Natl. Acad. Sci. USA 108, 6509–6514.
Uno, K.T., Polissar, P.J., Jackson, K.E., deMenocal, P.B., 2016a. Neogene biomarker record of vegetation change in eastern Africa. Proc. Natl. Acad. Sci. USA 113, 6355–6363.
Uno, K.T., Polissar, P.J., Kahle, E., Feibel, C.S., Harmand, S., Roche, H., deMenocal, P.B., 2016b. A Pleistocene palaeovegetation record from plant wax biomarkers from the Nachukui Formation, West Turkana, Kenya. Phil. Trans. R. Soc. B 371, 20150235.
Valla, P.G., Shuster, D.L., Van Der Beek, P.A., 2011. Significant increase in relief of the European Alps during mid-Pleistocene glaciations. Nat. Geosci. 4, 688–692.
Verschuren, D., Sinninghe Damsté, J.S., Moernaut, J., Kristen, I., Blaauw, M., Fagot, M., Haug, G.H., 2009. Half-precessional dynamics of monsoon rainfall near the East African Equator. Nature 462, 637–641.
Vogts, A., Moossen, H., Rommerskirchen, F., Rullkötter, J., 2009. Distribution patternsn and stable carbon isotopic composition of alkanes and alkan-1-ols from plant waxes of African ranf forest and savanna C_3 species. Org. Geochem. 40, 1037–1054.

Volkman, J.K., Barrett, S.M., Blackburn, S.I., Mansour, M.P., Sikes, E.L., Gelin, F., 1998. Microalgal biomarkers: a review of recent research developments. Org. Geochem. 29, 1163–1179.
Vrba, E.S., 1985. Environment and evolution: Alternative causes of the temporal distribution of evolutionary events. South Afr. J. Sci. 81, 229–236.
Vrba, E.S., 1993. Turnover-pulse, the red queen, and related topics. Am. J. Sci. 293, 418–452.
Webb, M., Barker, P.A., Wynn, P.M., Heiri, O., Van Hardenbroek, M., Pick, F., Russell, J.M., Stott, A.W., Leng, M.J., 2016. Interpretation and application of carbon isotope ratios in freshwater diatom silica. J. Quat. Sci. 31, 300–309.
Westover, K.S., Stone, J.R., Yost, C.L., Scott, J.J., Cohen, A.S., Rabideaux, N.M., Stockhecke, M., Kingston, J.D., 2021. Diatom paleolimnology of late Pliocene Baringo basin (Kenya) paleolakes. Palaeogeogr. Palaeoclimatol. Palaeoecol. 570, 109382.
WoldeGabriel, G., Ambrose, S.H., Barboni, D., Bonnefille, R., Bremond, L., Currie, B., DeGusta, D., Hart, W.K., Murray, A.M., Renne, P.R., 2009. The geological, isotopic, botanical, invertebrate, and lower vertebrate surroundings of *Ardipithecus ramidus*. Science 326, 65e1–65e5.
Wynn, J.G., 2000. Paleosols, stable carbon isotopes, and paleoenvironmental interpretation of Kanapoi, Northern Kenya. J. Hum. Evol. 39, 411–432.
Wynn, J.G., 2004. Influence of plio-pleistocene aridification on human evolution: Evidence from paleosols of the Turkana Basin, Kenya. Am. J. Phys. Anthropol. 123, 106–118.
Yellen, J., Brooks, A., Helgren, D., Tappen, M., Ambrose, S., Bonnefille, R., Feathers, J., Goodfriend, G., Ludwig, K., Renne, P., 2005. The archaeology of aduma middle stone age sites in the awash valley, Ethiopia. PaleoAnthropology 10, e100.